

GEORGIA INSTITUTE OF TECHNOLOGY
ENGINEERING EXPERIMENT STATION

Posted
as

PROJECT INITIATION

Date: June 3, 1975

Project Title: Location and Structural Role of Water in Tooth Enamel

Project No.: B-448

Project Director: Dr. Paul E. Mackie

Sponsor: PHS - Extramural Programs (NIH)

Agreement Period: From June 1, 1975 Until May 31, 1978

Type Agreement: Grant No. 1 R01 DE04151-01

Amount: \$50,039 PHS Funds
2,633 GIT (E- - -) Total \$52,672

Reports Required:

Interim Progress Report; Terminal Progress Report
Sponsor Contact Person:

Dr. Paul D. Frazier
Chief, Mineralization, Salivary Secretions & Nutrition Program
Extramural Programs
Public Health Service
Bethesda, Maryland 20014

Assigned to: PHYSICAL SCIENCES DIVISION

COPIES TO:

Project Director

Director, EES

Director, ORA/GTRI

Assistant Director

Division Chief

EES Accounting

Patent Coordinator

EES Supply Services

Photographic Laboratory

Security—Reports—Property Office

General Office Services

Library, Technical Reports Section

Office of Computing Services

Project File

Other

Sue Corbin, Bonnie Wettlaufer

GEORGIA INSTITUTE OF TECHNOLOGY
OFFICE OF CONTRACT ADMINISTRATION
SPONSORED PROJECT TERMINATION

Date: April 4, 1980

Project Title: Location and Structural Role of Water in Tooth Enamel

Project No: B-448-002

Project Director: Dr. Paul E. Mackie

Sponsor: PHS - Extramural Programs

Effective Termination Date: May 31, 1979

Clearance of Accounting Charges: May 31, 1979

Grant/Contract Closeout Actions Remaining:

NONE

- ☐ Final Invoice and Closing Documents
- ☐ Final Fiscal Report
- ☐ Final Report of Inventions
- ☐ Govt. Property Inventory & Related Certificate
- ☐ Classified Material Certificate
- ☐ Other _____

Assigned to: EML/SSD (~~School~~ Laboratory)

COPIES TO:

Project Director
Division Chief (EES)
School/Laboratory Director
Dean/Director-EES
Accounting Office
Procurement Office
Security Coordinator (OCA)
/ Reports Coordinator (OCA)

Library, Technical Reports Section
EES Information Office
Project File (OCA)
Project Code (GTRI)
Other _____

Final Report of Project B448

LOCATION AND STRUCTURAL ROLE OF WATER IN TOOTH ENAMEL

P. E. Mackie
Engineering Experiment Station
Georgia Institute of Technology
Atlanta, Georgia 30332

NIDR Grant No. DE 04151

8 January 1980

Prepared for:
National Institute of Dental Research
Bethesda, Maryland

Final Report for DE04151

Abstract

The primary goal of this work was to obtain an understanding of the occurrence, location, binding, variety, changeability, and functional role of the "water" in human tooth enamel in relation to various properties of human teeth.

The principal result of this study is that for the first time a direct refinement of the crystallographic details of human tooth enamel has been achieved. As a result, future atomic-scale models for the crystalline portion of human tooth enamel can be based on a more realistic model (which was experimentally determined directly on human tooth enamel itself) than the idealized model system of the past, hydroxyapatite. The crystallographic details of the scattering density along the "open-channel" of the apatite structure are consistent with some, if not most, of the water of tooth enamel being in this channel at $z \approx 0.12-0.14$ in a partially oriented state (e.g. "restrained tumbling"). Based on the current structure refinements (which need to be repeated with further improvements in the model, such as the inclusion in the model of such entities as CO_3 , HPO_4) water may be present in this channel at ~ 3.6 wt%.

Final Report
for
DE04151
(1 June 1975 - 31 May 1979)

A1. Introduction

Work on this project occurred in two fairly distinct phases. The first phase (i.e. Phase I) occurred from June 1975 to May 1977 and consisted of: 1) development of techniques, 2) the building of equipment and 3) the use of the above equipment and techniques to perform a first crystallographic structure refinement of the atomic-scale details of human tooth enamel (HTE). Due to the costliness of HTE these first trial structure refinements were necessarily made with enamel which had been collected some years before and was somewhat expendable due to its extended shelf life and lack of complete characterization. The results obtained from these initial efforts in Phase I permitted us to refine the techniques and improve upon the atomic-scale models utilized with our study of the better characterized (and more valuable!) HTE.

Phase II (June 1977 to May 1979) consisted of redoing some of the experiments done in Phase I but with better characterized enamel and, with the insight gained from Phase I, better experiment design (e.g. selection of more appropriate temperatures) and better techniques (e.g. closer monitoring of the quality of data obtained from the automated powder diffractometer which can significantly effect the results obtained with the PFSR method).

This final report is written to reflect the two phase nature of the work which was done. Phase I is reported in section A2 and Phase II in section A3.

A2. Phase I Progress Report:

A2a) Covering the period (1 June 1975 to 16 May 1977)*

A2b) Summary

During this initial grant period (DE04151-00,01, and 02), the work on understanding the occurrence, location, binding, variety, changeability and functional role of "water" present in human dental enamel progressed along six fronts. Major project activities were in the areas of: (i) acquisition of human teeth and the preparation of enamel powders, (ii) x-ray diffraction study (XRD) of powdered human tooth enamel, in vacuum, from 25°C to 500°C, (iii) thermogravimetric analysis (TGA) of a number of different enamel samples with different ages and particle sizes, (iv) infra-red analysis (i.r.) and dynamic evolved gas infra-red (DGIR) analysis of pyrolyzed enamel and the evolved products of pyrolyzed enamel respectively, (v) mass spectrometry (MS) of the gaseous products of pyrolyzed human tooth enamel, (vi) equipment design, fabrication and modification for the XRD, MS, TGA and DGIR experiments.

A major accomplishment during this report period was the substantial step forward in the direct study of human tooth enamel itself by the Pattern-Fitting-Structure-Refinement method (PFSR). This method, PFSR, applied to powdered human tooth enamel has provided for the first time quantitative structure analysis of the crystalline portion of tooth enamel, per se.

A2c) Detailed Report

Sample Acquisition and Preparation

The collection and preparation (see Method of Procedure for details of the preparation techniques) of whole sound human teeth, both age differentiated and pooled, has been a continuous activity during the first grant period. Approximately 2, 50, and 50 grams of TE powder have been prepared for the under 15 years, 16-50 years, and the 51 and over categories, respectively. Another 100 grams of enamel powder have been prepared from teeth with no age differentiation. These figures include both the heavy (sp. g. >2.95) and medium (2.95 > sp. g. > 2.84) density fraction. At the end of phase I, a backlog of about 200 whole teeth existed on which no work had been done yet.

X-ray Diffraction & PFSR of Human Tooth Enamel (TE)

A powder x-ray diffraction environmental chamber was designed and built. This chamber is capable of heating the sample to 500°C while maintaining the sample under a vacuum (see Figures 1 through 3). The design is such that gases evolved from the sample as it is pyrolyzed may be collected in an external glass vessel for further analyses (e.g., mass spectrometry). This chamber was also used to maintain the sample in controlled atmospheres (e.g., various humidities) in the second phase of this work.

*See Changes in Effort of the Summary Progress Report of the first project year. That section explains that full-time effort was delayed until January 1976. In addition, a 1/3 reduction in effort was required by the reductions made by Council in the personnel services of originally submitted budget.

This chamber was used to collect 14 x-ray diffraction data sets on a "pooled" enamel sample at 8 different temperatures from room temperatures to 500°C and then back to room temperature under vacuum (~ 20 milliTor) conditions. These 14 data sets have been analysed by the method of Pattern-Fitting-Structure Refinement (PFSR). Since PFSR is a relatively new technique (see "Application of the Pattern-Fitting-Structure-Refinement Method to X-ray Powder Diffractometer Patterns", R.A. Young, P.E. Mackie and R.B. Von Dreele, Journal of Applied Crystallography, (1977)) a short description is warranted at this point.

The method of PFSR entails using a computer program in conjunction with an atomic-scale model of the material under study to calculate an x-ray powder diffraction pattern. The atomic-scale model is defined by specifying where each atom is located (i.e., what are the x, y and z's of each atom) specifying how each atom is moving and by specifying the probabilities with which one would find a given crystallographically unique atom in a given unit cell. In addition to specifying parameters which describe the atomic model, one must specify other parameters which describe the "state" of the sample (e.g., crystallite size, strain, preferred orientation, etc.) and which describe the experimental setup (e.g., incident wavelengths or spectral distribution, instrumental resolution and aberrations). After everything is specified an x-ray powder diffraction pattern can be calculated. In practice, this calculated pattern will differ from the observed pattern. The parameters of the model (and experiment!) must then be adjusted or changed to make the calculated pattern fit the observed pattern better in a least-squares sense. In this manner (with a method quite similar to that used for single-crystal x-ray analyses) one can obtain directly crystal structure details of human tooth enamel. In practice, many cycles of refinement and much computer time are needed to gradually refine the atomic model (e.g., adding missing constituents of the model such as impurities, until the desired degree of fit is obtained).

The PFSR analyses of the 14 data sets described above have not been fully completed yet, but are far enough along so that some significant questions are answered, while still other questions were raised which have suggested additional experiments to be performed. So far, the positions and site occupancies of the calciums (Ca(1) and Ca(2)) and the atoms in the phosphate group (P, O(1), O(2) & O(3)) have been determined (see Table I). While there is evidence of significant changes in atomic details occurring along the hexad axis of the apatite-like structure as a function of temperature, the results obtained from the initial 14 data sets of phase I can not be interpreted conclusively for the atoms on this axis.

While not differing to a major degree, these results are based on the preliminary Phase I data, and differ in some atomic-scale details from the results obtained in Phase II (with better data) and reported in "Crystallography of Human Tooth Enamel: Initial Structure Refinement".

From Table I and Figure I one can see that the most obvious difference in structural parameters between TE and Holly Springs hydroxapatite is a rotation of the PO_4 groups about an axis which passes through the O_3 's. There is a slight increase in the size of the Ca_2 and O_3 triangles. The O_3 -P- O_3 angle is smaller in TE than in Holly Springs OHAp. Smaller-than-normal site occupancy factors for O_1 , O_2 and P relative to O_3 , suggests that there may be considerable disorder, in TE, of the PO_4 groups about the axis through the O_3 's perpendicular to the mirror planes. This hypothesis is further supported by additional PFSR refinements (incomplete at the end of Phase I) with isotropic temperature factors for the calciums and PO_4 groups allowed to vary, which reveal close-to-normal temperature factors for the O_3 and P but very much enlarged thermal factors for the O_1 and O_2 .

O ₁				
	x	y	z	s
TE	25°C	4073 _{2 5}	5222 _{3 7}	$\frac{1}{2}$.50 ₂
	185°C	4086 _{2 6}	5275 _{3 3}	$\frac{1}{2}$.41 ₂
	250°C	4058 _{2 6}	5266 _{3 2}	$\frac{1}{2}$.39 ₂
	300°C	4086 _{2 5}	5259 _{3 6}	$\frac{1}{2}$.48 ₂
	350°C	4129 _{2 5}	5321 _{3 6}	$\frac{1}{2}$.45 ₂
	400°C	4101 _{2 4}	5255 _{3 6}	$\frac{1}{2}$.49 ₂
	450°C	4109 _{2 5}	5287 _{3 7}	$\frac{1}{2}$.45 ₂
	450°C	4107 _{2 5}	5305 _{3 6}	$\frac{1}{2}$.45 ₂
	500°C	4090 _{2 7}	5243 _{4 0}	$\frac{1}{2}$.47 ₂
	500°C	4118 _{2 4}	5258 _{3 7}	$\frac{1}{2}$.46 ₂
	400°C	4104 _{2 5}	5282 _{3 7}	$\frac{1}{2}$.47 ₂
	300°C	4074 _{3 0}	5153 _{4 7}	$\frac{1}{2}$.49 ₃
	185°C	4065 _{2 4}	5232 _{3 5}	$\frac{1}{2}$.49 ₂
	25°C	4031 _{2 7}	5210 _{3 7}	$\frac{1}{2}$.44 ₂
OHAp	25°C	3282 ₂	4846 ₂	$\frac{1}{2}$

O ₃				
	x	y	z	s
TE	25°C	3448 _{2 9}	2651 _{1 9}	244 _{2 4} 1.05 ₃
	185°C	3531 _{2 3}	2697 _{1 7}	333 _{2 1} .92 ₂
	250°C	3557 _{2 1}	2717 _{1 6}	345 _{1 9} .90 ₂
	300°C	3427 _{3 0}	2668 _{1 9}	255 _{2 3} .97 ₃
	350°C	3488 _{2 6}	2689 _{1 8}	289 _{2 1} 1.01 ₂
	400°C	3419 _{3 0}	2664 _{1 9}	253 _{2 3} .96 ₂
	450°C	3471 _{2 7}	2683 _{1 8}	271 _{2 2} .99 ₂
	450°C	3492 _{2 6}	2685 _{1 8}	278 _{2 2} 1.01 ₂
	500°C	3459 _{3 1}	2674 _{2 0}	223 _{2 6} 1.01 ₃
	500°C	3411 _{2 9}	2654 _{1 9}	249 _{2 3} .96 ₂
	400°C	3439 _{2 9}	2657 _{1 9}	261 _{2 3} .98 ₃
	300°C	3531 _{2 8}	2673 _{1 9}	237 _{2 6} 1.13 ₃
	185°C	3413 _{3 0}	2656 _{1 9}	249 _{2 3} .98 ₂
	25°C	3460 _{2 7}	2657 _{1 8}	259 _{2 2} 1.01 ₂
OHAp	25°C	3433 ₁	2579 ₁	704 ₁

O ₂			
x	y	z	s
6633 _{4 1}	4738 _{4 3}	$\frac{1}{2}$.37 ₂
6512 _{3 8}	4676 _{4 0}	$\frac{1}{2}$.34 ₂
6553 _{3 6}	4729 _{3 7}	$\frac{1}{2}$.32 ₂
6610 _{4 1}	4766 _{4 0}	$\frac{1}{2}$.34 ₂
6603 _{3 9}	4767 _{3 9}	$\frac{1}{2}$.36 ₂
6585 _{4 0}	4746 _{3 9}	$\frac{1}{2}$.34 ₂
6585 _{4 1}	4716 _{4 0}	$\frac{1}{2}$.35 ₂
6651 _{3 8}	4772 _{4 0}	$\frac{1}{2}$.37 ₂
6559 _{4 8}	4678 _{4 8}	$\frac{1}{2}$.35 ₂
6646 _{4 2}	4784 _{2 6}	$\frac{1}{2}$.32 ₂
6540 _{4 5}	4669 _{4 4}	$\frac{1}{2}$.33 ₂
6652 _{4 6}	4733 _{5 0}	$\frac{1}{2}$.42 ₃
6608 _{4 2}	4719 _{4 1}	$\frac{1}{2}$.33 ₂
6596 _{4 2}	4723 _{4 2}	$\frac{1}{2}$.35 ₂
5876 ₁	4652 ₁	$\frac{1}{2}$	

P			
x	y	z	s
3973 _{2 5}	3525 _{2 4}	$\frac{1}{2}$.48 ₁
4000 _{2 0}	3586 _{2 0}	$\frac{1}{2}$.40 ₁
4002 _{1 8}	3605 _{1 7}	$\frac{1}{2}$.40 ₁
3953 _{2 4}	3573 _{2 3}	$\frac{1}{2}$.45 ₁
3987 _{2 1}	3584 _{2 1}	$\frac{1}{2}$.47 ₁
3947 _{2 4}	3563 _{2 3}	$\frac{1}{2}$.44 ₁
3962 _{2 2}	3568 _{2 2}	$\frac{1}{2}$.46 ₁
3993 _{2 1}	3576 _{2 1}	$\frac{1}{2}$.47 ₁
3970 _{2 6}	3521 _{2 6}	$\frac{1}{2}$.47 ₁
3939 _{2 4}	3549 _{2 3}	$\frac{1}{2}$.44 ₁
3950 _{2 4}	3569 _{2 3}	$\frac{1}{2}$.46 ₁
3984 _{2 7}	3474 _{2 7}	$\frac{1}{2}$.51 ₁
3950 _{2 4}	3536 _{2 3}	$\frac{1}{2}$.45 ₁
3971 _{2 2}	3532 _{2 2}	$\frac{1}{2}$.46 ₁
3983 ₁	3683 ₁	$\frac{1}{2}$	

Table I

		Ca _I						Ca _{II}			
		x	y	z	S			x	y	z	S
TE	25°C	1/3	2/3	256 ₂₁	.350 ₆			2492 ₁₁	9892 ₁₄	$\frac{1}{2}$.539 ₈
	185°C	1/3	2/3	228 ₂₁	.290 ₅			2485 ₁₀	9882 ₁₃	$\frac{1}{2}$.450 ₆
	250°C	1/3	2/3	231 ₁₉	.288 ₅			2477 ₁₀	9872 ₁₂	$\frac{1}{2}$.445 ₅
	300°C	1/3	2/3	305 ₁₈	.356 ₅			2471 ₁₁	9874 ₁₃	$\frac{1}{2}$.521 ₇
	350°C	1/3	2/3	292 ₁₈	.352 ₅			2473 ₁₀	9866 ₁₃	$\frac{1}{2}$.525 ₆
	400°C	1/3	2/3	301 ₁₈	.352 ₅			2472 ₁₀	9875 ₁₃	$\frac{1}{2}$.523 ₆
	450°C	1/3	2/3	297 ₁₈	.343 ₅			2472 ₁₀	9879 ₁₃	$\frac{1}{2}$.519 ₆
	450°C	1/3	2/3	286 ₁₉	.341 ₅			2468 ₁₀	9873 ₁₃	$\frac{1}{2}$.521 ₆
	500°C	1/3	2/3	293 ₂₁	.343 ₆			2476 ₁₂	9885 ₁₅	$\frac{1}{2}$.526 ₈
	500°C	1/3	2/3	301 ₁₈	.342 ₅			2469 ₁₀	9878 ₁₃	$\frac{1}{2}$.515 ₆
OHAp	400°C	1/3	2/3	290 ₁₉	.345 ₆			2482 ₁₀	9893 ₁₃	$\frac{1}{2}$.528 ₇
	300°C	1/3	2/3	248 ₂₃	.357 ₇			2490 ₁₂	9882 ₁₅	$\frac{1}{2}$.555 ₉
	185°C	1/3	2/3	308 ₁₈	.347 ₅			2474 ₁₁	9884 ₁₃	$\frac{1}{2}$.526 ₇
	25°C	1/3	2/3	263 ₁₉	.338 ₅			2484 ₁₀	9892 ₁₃	$\frac{1}{2}$.521 ₆
	25°C	1/3	2/3	013 ₁	.323 ₁			2465 ₁	9931 ₁	$\frac{1}{2}$.485 ₁

Table 1 (continued)

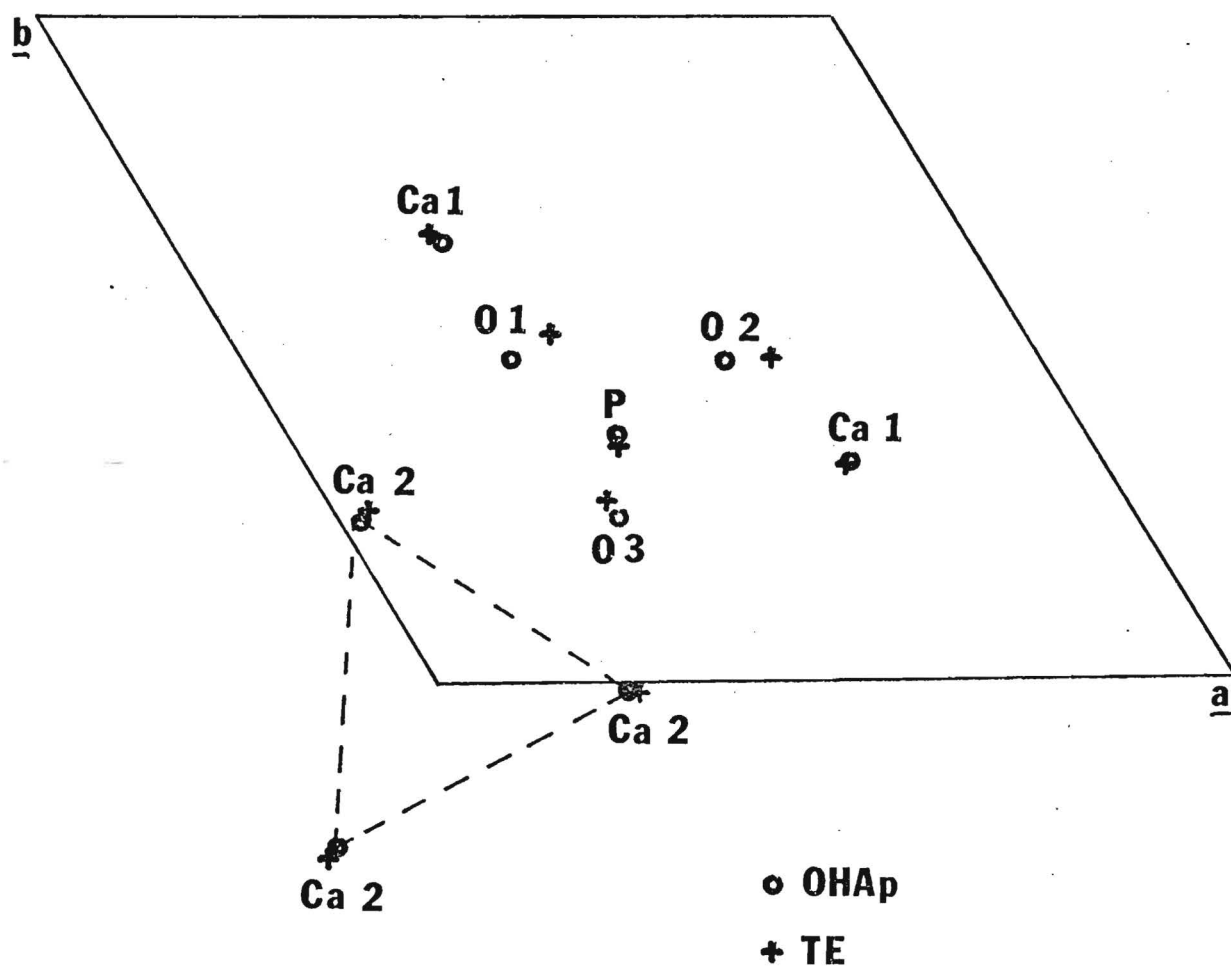


FIG. 1

Lattice parameters, obtained from the PFSR refinements of the 14 data sets, show that the a parameter undergoes a decrease from $\sim 250^\circ\text{C}$ and 350°C (see Figure 2). Note that these a values are for the crystal at the indicated temperature, not after being brought back to room temperature. One question raised by these results is why the room temperature a parameter is the same before and after pyrolysis at 500°C (this appears to contradict our own previous experiences and the results of others, e.g., see R.F. LeGeros, et al. "Types of 'Water' in Synthetic and in Human Enamel Apatites", IADR, Copenhagen, 31 March-31 April, 1977). However, this experiment differed from the others in that the sample was held in a vacuum at all times during the heating regimen. Further experiments during DE04151-02 (heating the sample in vacuum and in air) should clarify this situation.

When one plots the site occupancy factors (S) for the various atoms in TE vs temperature a curious decrease in the S's is observed in the temperature range 185°C to 250°C . This coincides both with (i) the temperature at which chlorapatite is known to undergo a phase transition and (ii) the principal loss of weight as seen with TGA (primarily water). This decrease in the S's precedes ($\sim 75^\circ\text{C}$) the observed decrease in the a lattice parameter. These decreased S values could be indicating increased disorder (dynamic or static) as a precursor to the loss of material "from the lattice" indicated by the decreased a.

During our early refinements with tooth enamel data, what appeared to be a micro-crystalline ($\approx 50\text{\AA}$) calcium-phosphate phase was observed as a residual background. What first brought our attention to this, was the lack of fit (particularly in "tail" regions of the Bragg reflections) in the angular regions of 30° to 36° , 38° to 41° , 46° to 53° , and 59° to 66° ($\lambda = 1.54$). Very broad ($\approx 5^\circ$ FWHM) diffraction peaks occur in these angular regions when an observed tooth enamel diffraction pattern is convoluted with a gaussian crystallite size function of 50\AA width at half maximum. This identification is not unique to apatite though, since other calcium-phosphates (e.g., $\text{Ca}_4\text{P}_2\text{O}_9$, octa calcium-phosphates, etc.) yield similar peaks in these regions when "smeared" by the same broadening function. It will be interesting to see if this apparent micro crystalline component is present and varies with age with the age-differentiated enamel samples. The PFSR computer program is presently being completely re-written (under DE 01912-14, Professor R.A. Young, PI) to correct many of its present problems. The resolution of the possibility of a bi-modal distribution of crystallite sizes in TE awaits this new PFSR program with its improved profile functions.

Thermogravimetric Analysis (TGA) of Human TE

In the TGA work on TE, the curves exhibit "peaks" or "breaks" only as changes in slope. With large particle size there is a sharp break in the TGA curve at $\sim 410^\circ\text{C}$. With smaller particle sizes the break at 410°C is smaller. For larger particle sizes, bits of sample are actually expelled from the weighing tray as the temperature is increased. This correlates with our i.r. observations that CO_2 is rapidly evolved at 350°C . Water, while it is given off continuously as TE is heated, is rapidly evolved in the temperature range 280°C to 360°C . Apparently the CO_2 (which is released from CO_3 , as IR analyses before and after pyrolysis show reduction--eventually to zero--of the CO_3 present in the TE specimens) and the water are unable to escape from the TE macro-structure at lower temperatures; but at higher temperatures breakdown of the TE macro-structure then releases them, sometimes explosively if the particles are large. This may relate to Dibdin's (1969) observation from BET measurements that the pore-surface area of TE increased

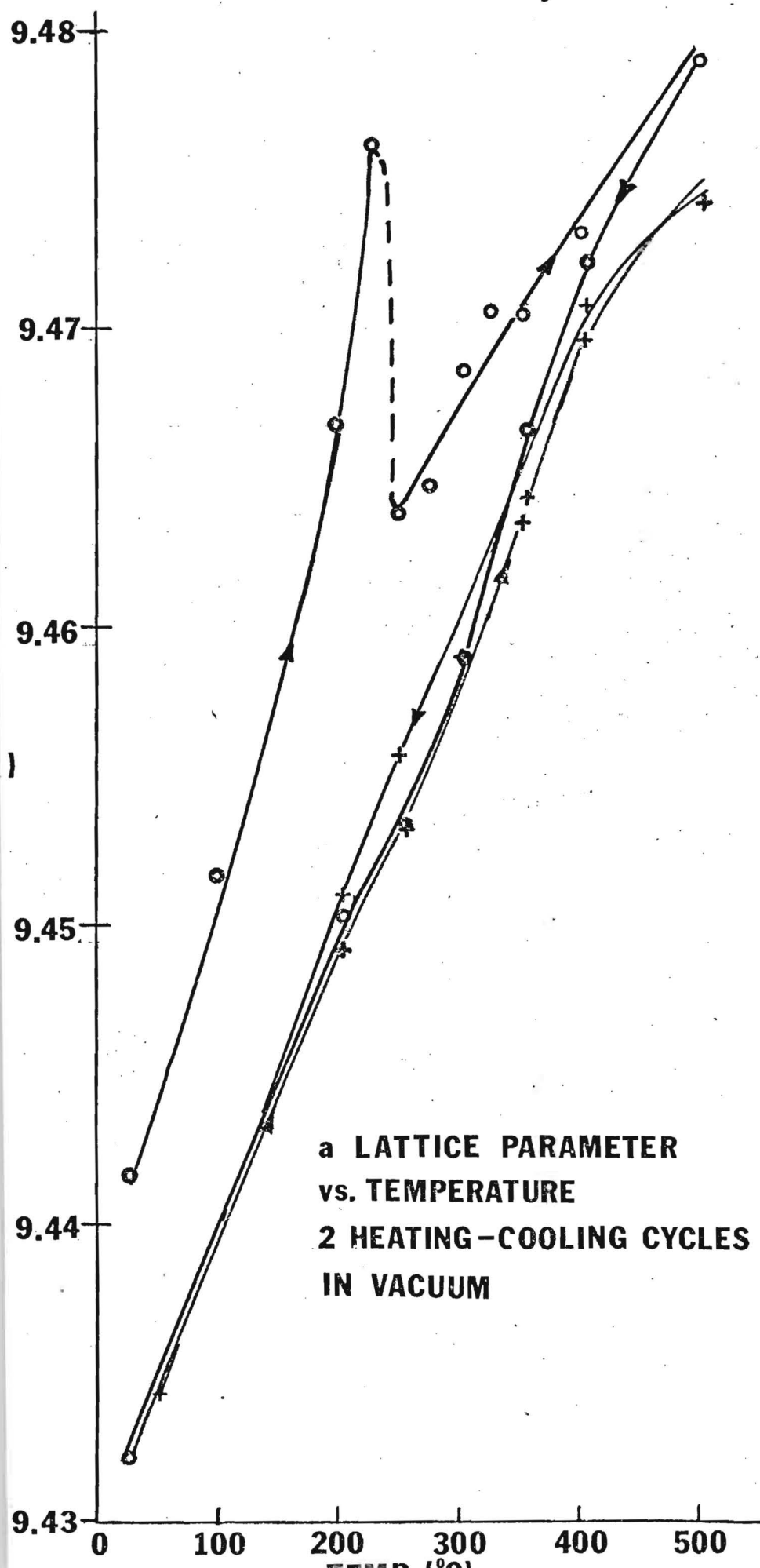


FIG. 2

fourfold at 360°C presumably because of pyrolysis of the organic content, and to Zahradnik and Moreno's (1975) observation with isothermal water vapour sorption measurements that the "pore constrictions" are associated with the presence of organic-matter "plugs". Modification of the sample holder (e.g., higher sides and a small mesh screen covering the top) resulted in a much smaller weight loss at 410°C. The fact that the "spalling" of TE material occurs at such a well defined temperature and also the fact that with sufficient reduction of particle size a sharp weight loss is no longer seen suggest the existence of characteristic cavities within TE macro-structure similar to the cavities of Dibdin or pores of Moreno and Zahradnik. Furthermore, these observations suggest that the water vapor pressure at 410°C (~ 3380 p.s.i.) is a measure of the mechanical strength either of the TE macro-structure or of the "organic plugs" in the pores suggested by Zahradnik and Moreno.

The first slope of the TGA is the steepest and occurs in the temperature range 25 to 200°C. Maximum slope and gas emissions occur at 115°C. This first rapid loss (up to 0.8wt%) is generally accepted to be H₂O and assumed to be that adsorbed on the organic and/or inorganic component. We have found:

- 1) for human TE samples heated to less than 150°C the weight loss can be regained by exposure to atmosphere.
- 2) for TE heated to less than 500°C (but more than 150°C) the weight lost in the 25°C to 200°C range can only be partially regained by exposure to atmosphere.
- 3) if TE is heated to 1000°C the 25°C to 185°C weight loss can not be regained even after prolonged (4 months) exposure to atmosphere, or even 1 week in H₂O.
- 4) even hydrothermal treatment (200°C @ 350psi for 225 hours in H₂O) will not totally restore the weight loss in the 25-200°C range for TE which has been heated to 500°C.
- 5) storage of TE for 4 months over P₂O₅ removes 65% of material normally lost by 200°C.
- 6) storage of TE for 14 days at 110°C in vacuum removes 80% of the material normally lost by 200°C.
- 7) a reflux preparation of hydroxyapatite shows a TGA weight loss (0-200°C) of 0.4wt%.
- 8) a hydrothermal preparation of hydroxyapatite (500°C @ 17000psi in H₂O) shows no TGA weight loss in the range 0°C to 200°C.
- 9) deproteination of TE with hydrazine eliminates 40% of the weight loss seen in the TGA curve of untreated TE by 200°C.
- 10) light fraction TE. (i.e., specific gravity <2.8) has a larger TGA weight loss than the heavy fraction up to 200°C (~ 1 wt%) but deproteination eliminates 60% of this weight loss from the TGA curve.

Eighty per cent of the weight loss below 200°C is probably due to adsorbed water; half of which is associated with the organic, the other half with the inorganic. By 200°C the organic material is starting to denature which inhibits its ability

PHOTOGRAPH LEGEND

Photo #1 Powder X-Ray Diffractometer and Environmental Chamber

1. Powder X-Ray Diffractometer
2. Environmental Chamber
3. X-ray Detector
4. X-ray Source

Photo #2 Close-up View of Sample Holder and Environmental Chamber Base-Plate

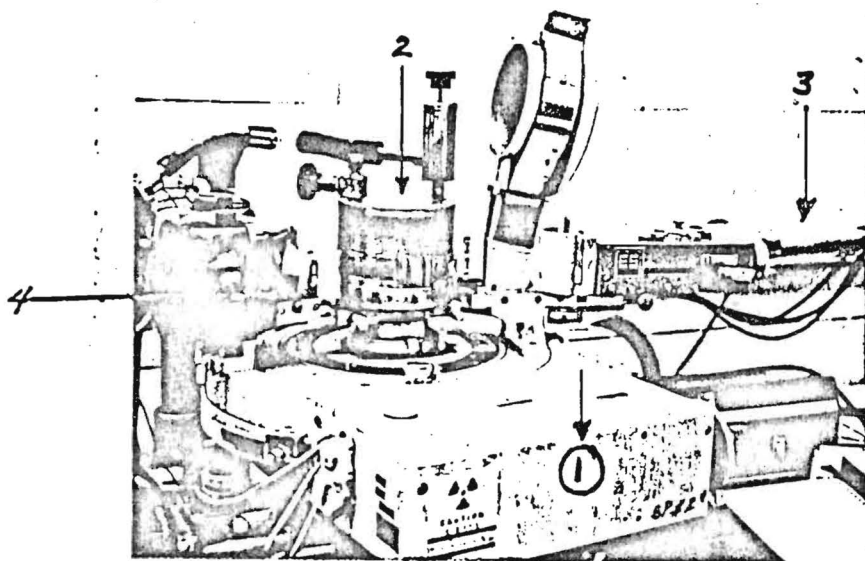
1. Powder Sample Holder with Heater Coils Imbedded
2. Water-cooled Base Plate
3. Adjusting Knob - to adjust position of sample in the x-ray beam
4. Wires for Heater Power and Thermocouple Readout

Photo #3 Environmental Chamber Base-Plate

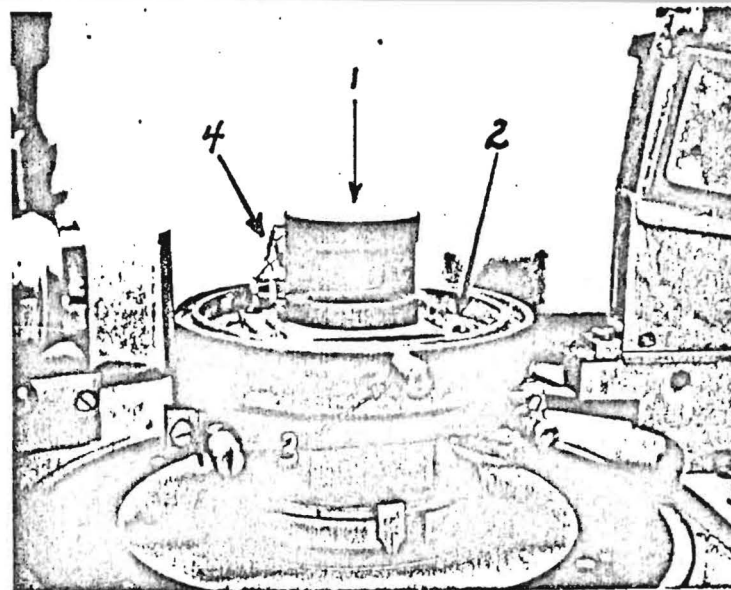
1. X-ray Source
2. Adjustable Platform on which Sample Holder is Positioned (see Photograph #2)
3. Connector Block for Heater-Power and Thermocouple Connections

Photo #4 Evolved Gas-IR Sample Holder

- 1 & 2. NaCl Windows - IR path is from 1 to 2
3. Heater Coil



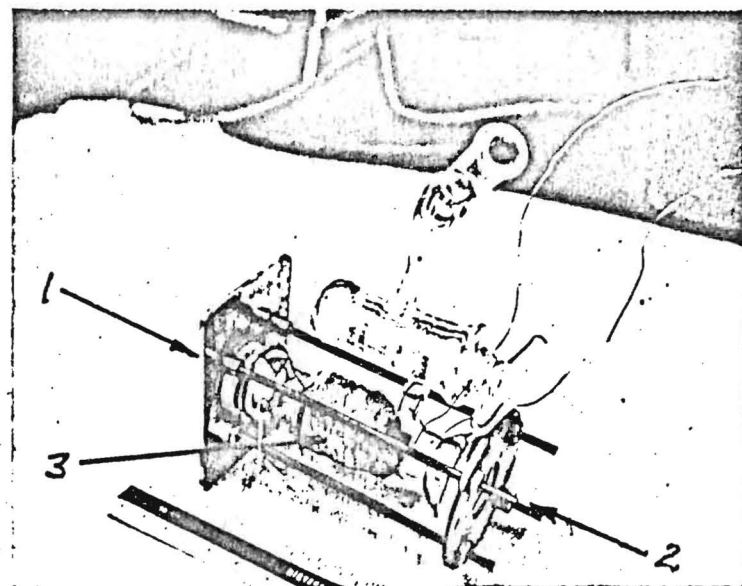
1
Powder X-Ray Diffractometer
and Environmental Chamber



2
Close-up View of Sample Holder and
Environmental Chamber Base-Plate



3
Environmental Chamber
Base-Plate



4
Evolved Gas-IR Sample Holder

to readsorb water. Heating TE to 400°C has a considerable charring effect (sample turns grey and organic gases are evolved) and eliminates the ability of the organic material to adsorb water. The water adsorbed on the inorganic material is similar to that adsorbed on the reflux prepared hydroxyapatite (prepared at 100°C).

The second slope in the TGA curves of TE starts around 300°C and extends to 1000°C with a small inflection noted at 780°C. This weight loss is associated with:

- i) water (from inorganic and organic components)
- ii) CO₂ (from both inorganic and organic components)
- and iii) several unidentified organic species.

This weight loss (i.e., from 300°C to 1000°C) has a maximum weight loss rate and maximum gas emissions (as determined from dynamic evolved gas IR experiments) at 390°C. By 390°C some 2.5wt% has been lost as seen by TGA measurements. This maximum emissions at 390°C correlates well with the explosive scattering of enamel chips (~400μ) observed at 410°C. Part of this 2% weight loss between 300°C and 1000°C is associated with the organic component as can be seen by:

- i) the sample slowly gets darker as the temperature goes from 300°C to 800°C; but then turns white again by 1000°C.
- ii) deproteinization decreases the weight loss in the range up to 900°C by ~1wt%.
- iii) organic gases (as seen by dynamic evolved gas IR) are evolved over the entire temperature range of 300°C to 1000°C.

This weight loss due to the organic components above 300°C is fairly continuous and hence has a smoothing effect on the TGA curve. CO₂ gas (2320cm⁻¹) is evolved starting at 200°C and is also fairly continuous. Changes in the IR spectra of the carbonate region point to the initially incorporated carbonate as the source of the evolved CO₂. The remainder of the 2wt% loss between 300°C and 1000°C is primarily water.

With the complementary use of evolved gas-IR we have established that assay for water in TE by TGA alone will be in serious error for at least two reasons:

1) Water is lost continuously and in combination with other entities as the temperature is raised, and

2) As much as 20% of the water in TE may not leave the enamel but becomes incorporated as structural OH in the apatite portion (e.g., see LeGeros, 1973, who showed structural OH increased with heating).

From this point of view, TGA although useful, is not our most valuable tool because of the complex nature of the weight loss. We have thus started using the dynamic evolved gas IR analysis technique to study the evolved gases of TE as they are given off. This should give us more accurate numbers for the H₂O lost (or other species!).

Mass Spectrometry (MS) of Human TE

Mass spectrometry of TE samples for H₂O and CO₂ is confounded by these same two entities which occur as background. Secondly, although the organic components are a small weight per cent of our prepared TE, organic vapors with complex fragmenting patterns are a high percentage of the total weight lost in a MS run and constitute a confusing background which needs to be removed in order to study the potentially small amounts of the entities of interest.

We performed step-wise heating regimens of TE for MS and dynamic evolved gas infra-red (DGIR) analyses. MS analysis was also being performed on evolved gases collected from the environmental chamber during x-ray powder diffraction runs.

The technique of step-wise heating and then the static analysis by the sector type mass spectrometer available to us did not fully meet the needs of this project. The gases were not analyzed as they were emitted (i.e., dynamically as the temperature was changed) but were collected in a glass vessel, while the sample was held at a constant temperature, to be analyzed at a latter time. This procedure suffered from a number of problems. First, the quantitative information was compromised because some of the gases tended to condense out on the cool walls of the collection vessel. This changed the ratios of the various gaseous species present in the gas to be eventually injected into the mass spectrometer. Secondly, with the mass spectrometer available to us, the injected gas had to follow a path with some bends in it before it arrived at the analyzing magnet. At each bend, the various gaseous species were removed from the gas stream (e.g., by condensation or scattering) to varying degree for each specie, further compromising the quantitative aspects of the data collected. A third problem was that those in charge of this instrument did not want us to inject gases at temperatures higher than about 300°C at the inlet. This was to reduce the possibility of contaminating the system with heavy organic mass fragments with a resulting costly down time to break open the vacuum system and thoroughly clean the system. A quadra-pole mass spectrometer, with its straight path through the system, would have reduced or eliminated the problems mentioned above. The gaseous effluents would be analyzed dynamically (i.e., on-line as the temperature is varied without the intermediate step of a collection vessel), the data collected would be more quantitative because of fewer opportunities for the gas stream to interact with various parts of the equipment along the path (it follows that the problem of contamination would also be reduced), and higher inlet temperatures for the injected gas would be feasible.

Several different possibilities for using quadra-pole type MS's were checked out. A Bendix time-of-flight unit in Ceramic Engineering needed repairs which would cost more than acquiring a new unit (~\$10000). A residual gas analyzer in the Physics department was in dedicated use and unavailable for use by this project. Similarly, use of a quadra-pole MS in the Areospace Engineering department was looked into. This unit was being used intensively and it was feared that injection of our biological samples at high temperatures would result in contamination and, hence, shut down the unit for extended lengths of time for cleaning.

To effectively acquire the dynamic (and quantitative) data of mass fragments vs temperature, a mass spectrometer, of the quadrapole type, would be desirable. Mass spectrometer identification of the various enamel effluents at each temperature has become more important with the result from dynamic evolved gas i.r. that the several evolved species are given off continuously and simultaneously. Good quantitative MS data would both complement and provide a check on the dynamic evolved gas i.r. results. For example, i.r. band assignments could be made by correlating changes in i.r. bands (e.g. changes in areas and shifts in position) with quantitative changes in the mass fragments of the MS output.

Infra-Red(IR) and Dynamic Evolved Gas IR (DGIR) of Human TE

With the realization that the TGA curves of TE were a composite of simultaneous continuous emissions of several species, the sample chamber (or cell) for continuous monitoring of the IR absorption bands of evolved gases was designed and built (see the next section: "Equipment Design, Fabrication and Modification"). Thus far, nine major absorption bands have been noted, as well as, many small peaks in the organic "Fingerprint" region ($600-1500\text{cm}^{-1}$). Efforts were directed toward calibrating the cell with pure oxalates in an effort to obtain weight loss vs temperature curves for each major specie evolved. This technique, DGIR, was investigated as a potential analytic assay for water. The only bands of the 9 assigned with certainty are H_2O and CO_2 which are the largest. Several other bands are assigned to at least two different organic species (one a gas and the other a condensed vapor).

Equipment Design, Fabrication and Modification

Several pieces of equipments were designed and built for DE04151. As mentioned in the section on x-ray diffraction, a sample environmental chamber (see Photos 1 through 3) was built to enable the sample to be heated up to 500°C while maintaining the sample in a vacuum or some control atmosphere. This chamber was used to obtain the TE (under vacuum) data vs temperature used in the PFSR studies. It was further used in DE04151-02 to maintain the sample at humidities other than ambient.

A special sample chamber (see photo #4) was constructed such that various species of the evolved gases could be monitored by IR continuously as the temperature of the sample was increased. This chamber has been used extensively in the dynamic pyrolysis studies of human TE (see R.A. Young et al. "Dynamic Pyrolysis Studies of Human Tooth Enamel", AADR, Las Vegas, June 1977).

A2d) Published Abstracts of Oral Presentations at Scientific Meetings

- i) "Experience with x-Ray PFSR: Profiles, LaPO_4 , and Tooth Enamel", P.E. Mackie, Dennis B. Wiles and R.A. Young, Program and Abstracts, American Crystallographic Association, Series II, 5 42, (1977).
- ii) "Preliminary Crystal Structure Analysis of Powdered Human Tooth Enamel", P.E. Mackie and R.A. Young, J. Dent. Res., 56, (Special Issue B), B 232 (1977).
- iii) "Dynamic Pyrolysis Studies of Human Tooth Enamel", R.A. Young, Derrold W. Holcomb and P.E. Mackie, J. Dent. Res., 56 (Special Issue B), B 233 (1977).

A3. Phase II Progress Report

A3a) Covering the period 17 May 1977 to 1 June 1979

A3b) Detailed Report

Previous sections of this progress report described 14 sets of x-ray powder diffraction patterns (collected at various temperatures) which were used with the then relatively new technique of Pattern-Fitting-Structure-Refinement. During the period May 1977 to Aug. 1977, 29 additional x-ray powder diffraction patterns were obtained of human tooth enamel held at various temperatures between 25°C and 500°C while held in a vacuum of ~10 to 20 millitorr. These data were collected with the environmental sample chamber especially designed and constructed for this task in Phase I. Collection of these 29 data sets is a repeat of the earlier experiment with 14 data sets which was performed in Phase I. However, the knowledge and experience gained from the previous experiment enabled us to design and perform the experiment better the second time around. For example, improved packing of the sample allowed the entire experiment to be performed (over a four month period) without having to repack the sample. Furthermore, the evidence of an irreversible thermal process occurring somewhere between 200° and 300°C (see Fig. 2 of this progress report) permitted us to judiciously select the temperature at which powder patterns were collected in order to enhance our chances of observing the crystallographic structure changes which may be occurring during that irreversible process. This one sample was allowed to equilibrate for at least 24 hours at each selected temperature (under a vacuum of ~20 microns) before the powder pattern was collected. These powder patterns were collected at several different temperatures, increasing in steps from 25°C to 500°C, with the step size being ~25°C in the vicinity of the irreversible process. In addition to these data at various temperatures, 9 powder patterns were obtained (during the period Sept. 1977 - March 1978) with the sample equilibrated and held at various relative humidities (the temperature maintained at 25°C). Data were collected with the sample in a dry atmosphere and in wet atmospheres with relative humidities (R.h.) ranging from 20% to 85% with approximately 10% steps in the R.h.

The 29 sets of data at various temperatures were initially used to perform PFSR analysis with the old PFSR program. A newer version of the PFSR program (with enhanced capabilities needed to improve the results obtained with such an analysis) has been under development for some time (under companion project DE01912) and has only recently become available. To the extent that such analyses are consistent with the goals of DE01912, it is expected that these analyses will be completed under project DE01912.

Results of a fairly substantial nature have already been obtained for the HTE data at room temperature. These crystallographic details of human T.E. are reported in a paper entitled "Crystallography of Human Tooth Enamel: Initial Structure Refinement" which has been accepted for publication in the Materials Research Bulletin. A preprint of this paper is enclosed.

Initial PFSR analyses (with the older PFSR program) of the data sets at the extremes of the humidity range employed have not yet allowed us to detect differences in the crystallographic details which could be construed to be statistically significant. Future PFSR refinements with the new version of PFSR (presumably on project DE01912) may yet yield detectable differences in crystallographic details in humidified vs non-humidified human tooth enamel.

A3c) Results

For the first time, the crystal structure details of enamel have been determined directly by powder x-ray diffraction and profile-fitting-structure-refinements. While the atomic-scale models employed were far from complete, some useful interpretations of the results can still be made at this time.

1) As suspected (due to the similarity of the powder patterns for HTE and hydroxyapatite), the crystal structure details of HTE are very much like OHAp. However, significant differences do exist. These differences show up primarily in the contents of the "X-ion" channel and the position and occupancy of the PO_4 groups.

2) The "X-ion" channel scattering density is consistent with a model which has ~ 3.6 wt% water, partially oriented at $z \approx 0.12 - 0.14$.

3) The disturbance of the phosphate oxygens has not been explained yet with any particular refined crystal structure model, but it may be possible with future refinements to account for such distortions with a model which includes CO_3 and HPO_4 substitutions.

A3d) Talks & Paper Since the Last Progress Report

A42. Papers Accepted for Publication

"Crystallography of Human Tooth Enamel: Initial Structure Refinement", R.A. Young and P.E. Mackie, accepted for publication in Materials Research Bulletin (1979).

A4b. Papers Presented at Meetings

1. "Pattern-Fitting-Structure-Refinement ('Profile Refinement') with X-Ray Powder Diffraction Data", R.A. Young, P.E. Mackie and D.B. Wiles, Conf. on Diffraction Profile Analysis, Krakow (1978).
2. "Crystallographic Changes Induced in Human Tooth Enamel By Moderate Heating", P.E. Mackie and R.A. Young, IADR meeting, New Orleans (1979).
3. "Flat and False Minima in Rietveld Crystal Structure Refinement of Human Tooth Enamel", R.A. Young, D.B. Wiles and P.E. Mackie, ACA, Honolulu (1979).

Paul E. Mackie
Senior Research Scientist

8 January 1980

PATTERN-FITTING-STRUCTURE-REFINEMENT ('PROFILE REFINEMENT')
WITH X-RAY POWDER DIFFRACTION DATA

R. A. Young, P. E. Mackie and D. B. Wiles

School of Physics and Engineering Experiment Station

Georgia Institute of Technology

Atlanta, Georgia 30332 U.S.A.

The pattern-fitting-structure-refinement (PFSR) method, best known as Rietveld's 'profile-refinement' method for neutron diffraction powder patterns, has only recently been applied to x-ray diffraction powder patterns (Malmros and Thomas, J. Appl. Crystallogr. 10, 7-11 (1977); Young, Mackie & von Dreele, ibid. pp. 262-269; Khattak & Cox, ibid. pp. 405-411). Structure refinements with x-ray powder data have been carried out on materials in at least six different space groups and with up to 28 adjustable parameters. As is also true for the neutron case, remarkably precise lattice parameters are a by-product. Whole-pattern R values, R_p , are similar to those obtained with neutron data (e.g., 10-30%) and atom position parameters agree with single crystal results, where available. Site occupancy and, especially, temperature factors so far obtained are less reliable, at least in part because of inadequate profile functions.

Proving its worth by application to a natural material that could not possibly be available in single crystal form, the x-ray PFSR method has provided the first crystal structure refinement of human tooth enamel, per se. Some significant differences from hydroxyapatite are shown, even though the results are preliminary because the model (hydroxyapatite with some Cl, F, and C substitutions) is not sufficiently complex and because better profile functions are needed. Further, useful results have been obtained on both reversible and irreversible structural-parameter changes occurring in the tooth enamel as it was cycled repeatedly between room temperature and 500°C (refinements at 7 to 10 temperatures on each cycle) and with different humidities.

Unlike the usual neutron diffraction profile, x-ray diffraction profiles are not well represented by Gaussian functions. The cited works have involved Gaussian, Lorentzian, and two-modified Lorentzian forms for the diffraction profiles. Which is better depends on the extent of diffraction and instrumental broadening present; all appear to be far from ideal. Thus, reliable site occupancy and temperature factors, desired sensitivity to

subtle structural differences, and exploitation of the full potential of the PFSR method await the use of more appropriate profile functions.

Other desired features of a good PFSR computer program include simultaneous refinement of two or more phases, improved handling of background including any amorphous contribution, capability for stripping out the total pattern of a major phase to permit concentration on a minor phase present, modular construction, portability, and immediate applicability to all space groups without need for special programming. A computer program meeting most of these objectives is now nearing completion.

This work has been supported in part by the U.S. Public Health Service through NIH-NIDR Grant DE-01912.

FLAT AND FALSE MINIMA IN RIETVELD CRYSTAL STRUCTURE
REFINEMENT OF HUMAN TOOTH ENAMEL. R.A. Young, D.B. Wiles and
P.E. Mackie, School of Physics and Engineering Experiment Sta-
tion, Georgia Institute of Technology, Atlanta, GA 30332

The Rietveld method of utilizing all information in a powder pattern to do crystal structure refinement, remarkably successful with neutron data, is beginning to produce important results with x-ray powder data. Experiences with human tooth enamel (TE) and related apatites suggest, however, that the method is less than ideally effective because of "flat" and false minima. "Flatness" is shown by relative insensitivity of R_{wp} to changes in atom positions and site occupancies. A test with a well known structure, fluorapatite, showed that displacing one oxygen atom by (only) $\sim 0.8\text{\AA}$ allowed it to be trapped in a false minimum which, in this case, could be distinguished from the true minimum on the basis of R_{wp} values (21% vs 14%). The problem is compounded by factors leading to rather high final R_{wp} values, such as deficiencies in the TE structural model which omits CO_3 (2-4 wt%) and H_2O (3-5 wt%) at as yet unknown locations. With TE, R_{wp} was about $26\pm 1\%$ whether or not the one atom was misplaced by 0.8Å. A similar flatness problem occurred with CO_3 substituting on the hexad axis of synthetic apatite.

M.J. Cooper noted (1978) that the σ 's are calculated too small, in principle. With TE and apatites, our positional σ 's are typically 0.01 to 0.02 Å but comparison of results from different data sets suggest that the true σ 's may be 2 to 3 times as large. Further, in thermally cycled TE apparent shifts in atom position differed up to 0.08Å with different Rietveld refinement programs and the same data set.

We conclude that when the structural model is not entirely correct, as ordinarily will be the case when one is trying to work out the actual detailed structural composition of a natural material, if R_{wp} does not fall below about 20% (1) one should expect the actual σ 's to be 2, 3, or more times those calculated and (2) false minima may be prevalent and undistinguished from the true minima.

This work was supported in part by NIH-NIDR Grants DE-01912, DE-04151.

R.A. Young (404) 894-5203

Key idea sentence: Applications of the remarkably successful Rietveld method are becoming sufficient to permit identification of some of its limitations.

Oral presentation

FORM A
INTERNATIONAL ASSOCIATION FOR DENTAL RESEARCH
and
AMERICAN ASSOCIATION FOR DENTAL RESEARCH

ABSTRACTS MUST BE RECEIVED BY OCTOBER 16, 1978

Complete: Items 1—5 below and type abstract within box, following instructions on reverse side.
Submit: Form A—Original and 4 Xerox copies; Form B—2 originals.

TYPE PERFECT ORIGINAL OF ABSTRACT HERE
 (Do not type beyond outline of box)

1. Full Name and Address of Author who will present paper:

Dr. P.E. Mackie
 Engineering Experiment Station
 Georgia Institute of Technology
 Atlanta, Georgia 30332

2. Mode of presentation:

- ☒ oral presentation only
☒ read by title acceptable
☐ poster presentation only
☐ oral or poster mode acceptable

3. Do you wish to withdraw your paper if it

- ☐ is placed in a mode not of your choosing?

GROUP CLASSIFICATION

- | | |
|--|---|
| <input type="checkbox"/> Behavioral Sciences | <input type="checkbox"/> Neuroscience |
| <input type="checkbox"/> Cariology | <input type="checkbox"/> Periodontal Research |
| <input type="checkbox"/> Craniofacial Biology | <input type="checkbox"/> Pharmacology |
| <input type="checkbox"/> Dental Materials | <input type="checkbox"/> Therapeutics, Toxicology |
| <input type="checkbox"/> Microbiology, | <input type="checkbox"/> Prosthodontics |
| Immunology | <input type="checkbox"/> Pulp Biology |
| <input checked="" type="checkbox"/> Mineralized Tissue | <input type="checkbox"/> Salivary Research |

SUBJECT CLASSIFICATION

- | | |
|---|--|
| <input type="checkbox"/> Anatomy | <input type="checkbox"/> Nutrition |
| <input type="checkbox"/> Biochemistry | <input type="checkbox"/> Oral Medicine |
| <input type="checkbox"/> Cell Biology | <input type="checkbox"/> Oral Surgery |
| <input type="checkbox"/> Chemistry | <input type="checkbox"/> Orthodontics |
| <input type="checkbox"/> Education | <input type="checkbox"/> Pathology |
| <input type="checkbox"/> Embryology | <input checked="" type="checkbox"/> Physics |
| <input type="checkbox"/> Endocrinology | <input type="checkbox"/> Physiology |
| <input type="checkbox"/> Endodontics | <input type="checkbox"/> Preventive Dentistry |
| <input type="checkbox"/> Enzymology | <input type="checkbox"/> Radiology, Radiobiology |
| <input type="checkbox"/> Epidemiology-Biostatistics | <input type="checkbox"/> Restorative Dentistry |
| <input type="checkbox"/> Genetics | <input type="checkbox"/> Temporomandibular Joint |
| <input type="checkbox"/> Health Services | <input type="checkbox"/> Tissue Culture |
| <input type="checkbox"/> Histology | <input type="checkbox"/> Ultrastructure |

☐ Other _____

Crystallographic Changes Induced In Human
 Tooth Enamel By Moderate Heating.
 P.E. MACKIE* and R.A. YOUNG. Georgia
 Institute of Technology, Atlanta, GA 30332

These changes were determined by full-pattern least-squares structure refinements (Rietveld method). The 29 X-ray powder patterns used, all of the dense portion of human tooth enamel, were collected "at temperature" throughout two 25-500°C heating cycles in vacuo. Irreversible changes now found to accompany the previously known contraction of the a axis (9.44 to 9.42Å) at ~200°C are (1) a 0.04Å shift in the 0(3) position bringing it approximately to the 0(3) position of hydroxyapatite, and (2) a decrease in the coefficient of the lattice thermal expansion (25-200°C) in the a direction from 17×10^{-6} to $11 \times 10^{-6}/^{\circ}\text{C}$ (cf. 12×10^{-6} unpublished dilatometric results of Barton for blocks of whole enamel, quoted by Bowen, Barton, and Mullineaux (1972), Dent. Mat. Res. NBS Special Publication No. 354, p. 97). The other atomic positions are unchanged within the expected experimental errors ($0.01\text{\AA} < \sigma < 0.05\text{\AA}$). It would seem that at least the outer few atomic layers of a caries site prepared with grinding or other abrading methods must have received the moderate heating required to produce these irreversible changes.

This work has been supported in part by NIDR Grants DE-01912 and DE-04151.

6. Reviewer's Rating:

<input type="checkbox"/>	<input type="checkbox"/>	<input type="checkbox"/>	<input type="checkbox"/>	<input type="checkbox"/>
1	2	3	4	5

7. Disposition:

<input type="checkbox"/>	<input type="checkbox"/>	<input type="checkbox"/>	<input type="checkbox"/>	<input type="checkbox"/>
O	P	T	R	W

CRYSTALLOGRAPHY OF HUMAN TOOTH ENAMEL: INITIAL STRUCTURE REFINEMENT

R.A. Young and P. E. Mackie
School of Physics and Engineering
Experiment Station
Georgia Institute of Technology
Atlanta, Georgia U.S.A.

13 March 1979

29 June 1979

30 October 1979

CPB Publication No. 82

Note:

This is a draft of a paper being submitted for publication. Contents of this paper should not be quoted nor referred to without permission of the authors.

CRYSTALLOGRAPHY OF HUMAN TOOTH ENAMEL: INITIAL STRUCTURE REFINEMENT

R.A. Young and P.E. Mackie
School of Physics and
Engineering Experiment Station
Georgia Institute of Technology
Atlanta, Georgia 30332 U.S.A.

ABSTRACT

A first crystal structure refinement of human tooth enamel, *per se*, has been achieved. For this, both x-ray and neutron powder diffraction data were analyzed with the Rietveld method of whole-pattern fitting. The dense fraction (sp.g. >2.95) of pooled human tooth enamel was used. Refinement in space group $P6_3/m$ led to $a = 9.441(2)\text{\AA}$, $c = 6.878(1)\text{\AA}$ and locations of the principal atoms similar to those in hydroxyapatite. The observed scattering density distributions along the hexad axis, including the differences between x-ray and neutron measures, would accommodate H_2O in some orientational disorder centered at $z = 0.11$ to 0.14 and the known small quantity of Cl^- ions partially substituting for OH^- (e.g. 1 in 20). This structure refinement constitutes the first direct evidence of both similarity and differences in the atomic-scale structural details of hydroxyapatite and human tooth enamel.

Introduction

Until now, no direct crystal structure analysis of human tooth enamel, nor any biological apatite, has been possible. That is because single crystals of size adequate for single-crystal structure analysis, by x-ray or neutron diffraction, do not exist. Hydroxyapatite, $\text{Ca}_5(\text{PO}_4)_3\text{OH}$ (Fig. 1), has customarily been taken as the model structure for human tooth enamel (TE) and other biological apatites. This inference of crystal structural similarity between hydroxyapatite (OHAp) and TE has been based on the similarity of their x-ray powder diffraction patterns (1). But neutron diffraction patterns are not as similar (2). Chemical analysis of TE shows significant amounts of elements not present in OHAp. Pyrolysis studies (3,4) show substantial differences. Infrared spectroscopic studies (5) and deuterizability studies (6) show real differences. Some of these evidences of difference between OHAp and TE have been reviewed recently (7). The strong conclusion is that, while the basic TE structure is somewhat similar to that of OHAp, there are many differences of detail to be expected and those differences are probably the most biologically important aspects of TE. Thus, direct crystal-structure refinement of TE, itself, is greatly to be desired.

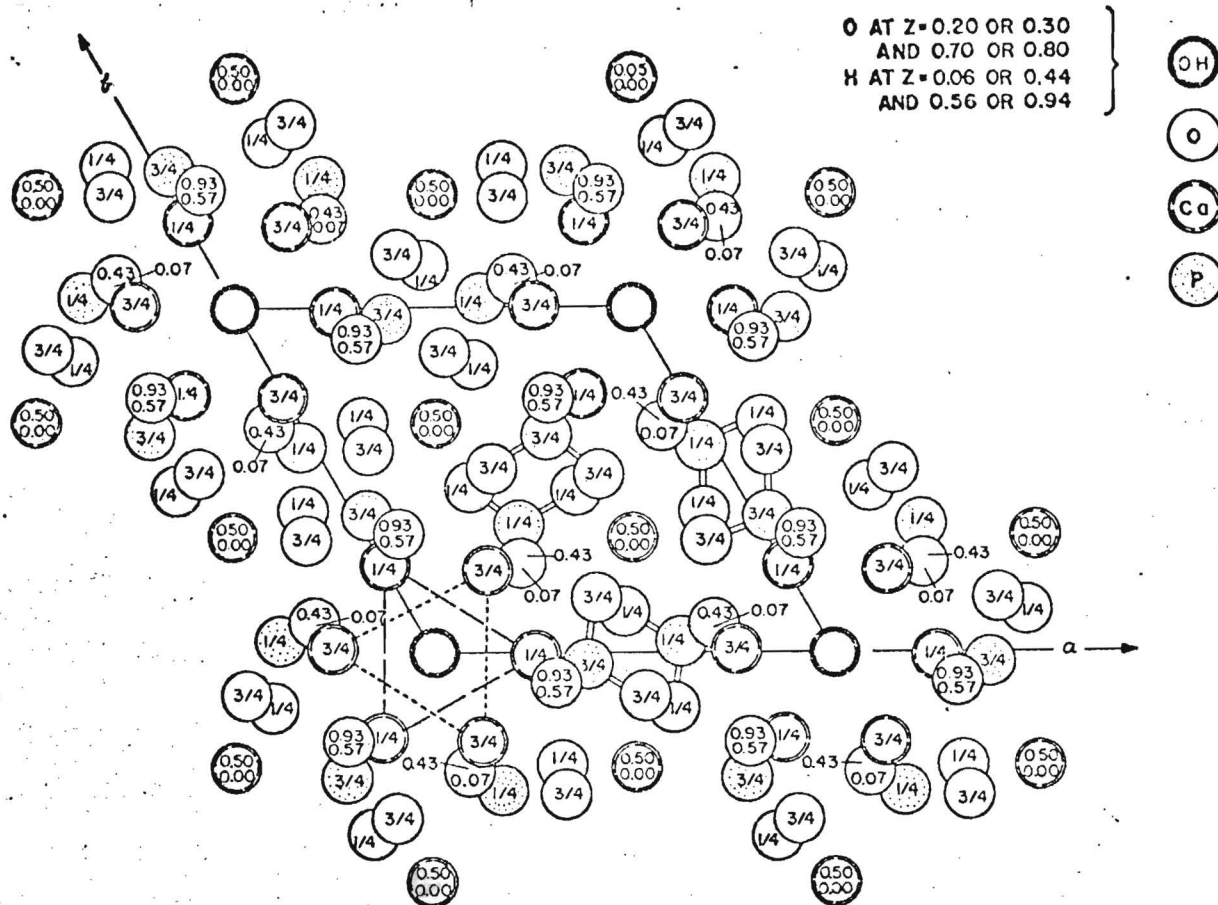


FIG. 1

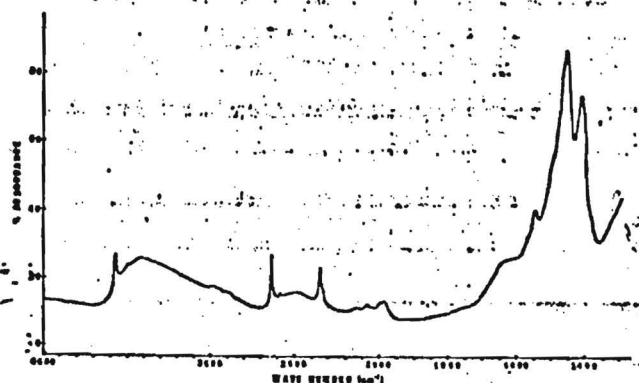
Hydroxyapatite structure (20). The numbers printed on the atom symbols are the z co-ordinates. The OH groups form a column at $x=0, y=0$; an "X-ion column". In $P6_3/m$ hydroxyapatite the OH is in two fold disorder about the mirror planes at $z=1/4$ and $z=3/4$ with O(H) at $z=0.19$ and the symmetry related positions with H about 1.0\AA further away from the mirror plane in each case.

Materials & Methods

The specimen material was the dense portion (sp.g. >2.95) of adult human tooth enamel. Because of the amount needed, the harvests from many teeth were pooled. The teeth, obtained from local dentists, were burnished with a dental burr to remove the pellicle, carious portions were excised, and the dentine was ground away from the inside. The resulting shells were then crushed to $<420\text{ }\mu\text{m}$ size and material of average density less than 2.95 g/cm^3 was floated off in tetrabromoethane. The dense portion was washed in 75% ethanol, dried in vacuum and air, and examined with a low power microscope in u.v. light. Those particles seen to fluoresce were discarded. The remainder was ground with a ruby mortar and pestle to pass through a $37\text{ }\mu\text{m}$ screen and was stored in air-filled vials while awaiting use. TE specimen sizes were typically about 0.5 gm for the x-ray work and $6\text{--}10\text{ gms}$ for the neutron work.

The specimens for neutron diffraction were further prepared by deuteration. After 13 days in D_2O at $200^\circ C$ and 225 p.s.i. pressure, i.r. showed that $\sim 50\%$ of the structural OH (that on the 6_3 axis) had been exchanged (Fig. 2).

FIG. 2



Portion of infrared spectrum of the partially deuterated tooth enamel used for the neutron diffraction data. The ratio of area under the OH-stretch frequency peak at 3572 cm^{-1} to that under its OD counterpart at 2636 cm^{-1} indicates the degree of deuteration to be $\sim 51\%$.

The x-ray data were obtained in digitized form with $CuK\alpha$ radiation and a standard Siemens x-ray powder diffractometer equipped with a diffracted-beam monochromator and operated in a step-scan mode. The x-ray data used in the structure refinements thus consisted of the intensities observed at each of these steps. Customarily, the step size was $0.05^\circ(2\theta)$ and the counting time per step was 60 seconds.

The neutron powder diffraction data were also obtained with a step-scan procedure (step size $0.05^\circ(2\theta)$) and a crystal-monochromated (111 of Cu) thermal neutron flux from the Georgia Tech Research Reactor operating at 1 MW. The monochromator 2θ angle was $\sim 72^\circ$, giving an adjusted neutron wavelength, λ , of $\sim 2.51\text{ \AA}$. A pyrolytic graphite filter was used to remove $\lambda/2$.

With both x-ray and neutron data the background was visually estimated on a plot of the data and was digitally subtracted, so that only net intensities were used in the structure refinements. With the exception of the neutron diffraction pattern, in which interfering $A\lambda$ peaks (due to the sample holder) had to be removed at $65.5^\circ(2\theta)$ and $77.5^\circ(2\theta)$, there were no interfering second phases in evidence, and it was not necessary to omit any other portions of the diffraction patterns. The 2θ ranges covered by the data were, approximately, 17° to $80^\circ(2\theta)$ (1260 points) for the x-ray data and 15° to 121° (1060 points) for the neutron data. (The neutron data collected at adjacent 0.05° increments were summed to yield data in 0.10° increments.)

The computer programs used for the structure refinements were (i) basically the Rietveld program (8) extended to be applicable with x-ray data as well as neutron data, as described by Young, Mackie and Von Dreele (9) and (ii) a newly written program with several improvements over the earlier ones (10). Initially, program (i) was used for both the x-ray and the neutron cases, but when (ii) became available for the x-ray case it was used in preference and all x-ray results reported here are those finally obtained with it. Gaussian profiles were used, in both the x-ray and the neutron

cases, to represent the individual reflection profiles. The profile width H was varied according to

$$H^2 = U \tan^2 \theta + V \tan \theta + W \quad (1)$$

where U , V and W are constants whose values were refined in the process. In the neutron case, the wavelength was known only approximately from the experimental geometry and, hence, it was adjusted incrementally between the various refinement runs. Also simultaneously refined in both cases were a 2θ -zero adjustment, the lattice parameters a and c , an overall temperature factor B , and positional parameters and site occupancies. Individual anisotropic temperature factors were fixed at their values in hydroxyapatite except for Cl and F which were fixed at their values in chlorapatite and fluorapatite, respectively. The sources of the x-ray atomic scattering factors used for Ca^{2+} , O^{1-} , F^{1-} , Cl^{1-} and $(\text{OH})^{1-}$ were obtained from the International Tables for X-ray Crystallography (11) and that for P^{1+} was interpolated from data obtained from the same source. Anomalous dispersion corrections (12) were applied. In the refinements with neutron data the scattering lengths used were, in units of $\text{cm} \times 10^{-12}$, 0.49 for Ca, 0.53 for P, 0.577 for O, and 0.99 for Cl, as given by Bacon (13). Although these values are not the latest (e.g. 0.47 is now known to be better for Ca), they suffice for this initial study; only the n 's (Table 1) of Ca are affected.

The starting model for the structure refinement was basically hydroxyapatite, space group $\text{P6}_3/\text{m}$, (Fig. 1) with the parameters given by Sudarsanan and Young (14) for their specimen X-23-10. No accommodation was provided in the model for CO_3 or H_2O , *per se* (determination of that degree of detail is still premature), but an effort was made to get an estimate of the distribution of scattering density (i.e. atoms of whatever kind) along the 6_3 axis, where position parameters are $0,0,z$. This is the region referred to variously as the X-ion region (15) or a "channel" (16). This estimate was obtained from refinements of five distinct models which differed only in the X-ion region, as follows:

	<u>X-Sites in model</u>	<u>z_1</u>	<u>z_2</u>	<u>z_3</u>	<u>Variables</u>
1)	O(H)	0.198	-	-	z & n
2)	O(H), Cl	0.198	0.390	-	n_1 & n_2
3)	X_1 X_2 X_3	0.00	0.10	0.20	n_1 n_2 n_3
4)	X_1 X_2 X_3	0.05	0.15	0.25	n_1 n_2 n_3
5)	X_1 X_2	0.198	0.444		n_1 n_2

Here " n " is the site occupancy parameter. The x-ray refinement used slightly different z values in model 2, $z=0.195$ & 0.400 . The difference between model 2 and model 5 is the expected quantity-dependent difference for the Cl position, 0.39 being expected in TE (17). Model 5 was refined only with the neutron data. Attempts to refine the two z parameters in model 2 with the x-ray data resulted in their moving toward each other until they and their associated site occupancies became so correlated as to abort the refinement. Hence the strategy of fixing positions and refining only site occupancies was used. Ideally one would like to fix such scattering sites at very close intervals all along the 6_3 axis and the refinement of the n 's would then provide a fine-scale histogram of the distribution of scattering density along the axis. The closeness with which these sites can be spaced is, however, limited by the $(\sin \theta)/\lambda$ range of the data in the direction of that line.

In the present cases the data range is so restricted (for various reasons not easily overcome) that a minimum spacing of about 0.1 c was the limit. Models 3 and 4, in which the X sites of one model are midway between those of the other, were therefore used to circumvent partially this difficulty.

In the refinement process, the quantity being minimized is

$$\sum w_i (y_i(\text{obs}) - \frac{1}{c} y_i(\text{calc}))^2, \quad (2)$$

where y_i is the net intensity at the i^{th} step in the scan of the powder diffraction pattern, w_i is the weight assigned to that observation (based on counting statistics, only, with the background variance included) and c is a scale factor. Hence, of the three "R factors" calculated by the computer program, the most significant is the weighted pattern one,

$$R_{wp} = \left[\frac{\sum w_i [y_i(\text{obs}) - \frac{1}{c} y_i(\text{calc})]^2}{\sum w_i (y_i(\text{obs}))^2} \right]^{1/2}. \quad (3)$$

On the basis of the refined results, the locally modified Rietveld program also allocates intensity among the overlapped reflections and produces pseudo-equivalents to observed Bragg intensities, I_B , which then can be used to form a conventional - but less significant - R-factor:

$$R_B = \frac{\sum |I_B(\text{obs}) - I_B(\text{calc})|}{\sum I_B(\text{obs})}. \quad (4)$$

The third R-factor calculated is, R_p , the unweighted pattern R-factor:

$$R_p = \frac{\sum |y_i(\text{obs}) - \frac{1}{c} y_i(\text{calc})|}{\sum |y_i(\text{obs})|} \quad (5)$$

Results

The principal results are shown in Figs. 3 & 4 and in Tables 1 & 2. The lattice parameter differences between TE and OHAp (hydroxyapatite) are already well known. Although the R_{wp} values are somewhat higher than is desirable, the sizes of the standard deviations suggest that the refinements should be useful in so far as they go. Fig. 3 shows how well the diffraction patterns calculated from the refined models agree with the observed patterns. With both the x-ray data and the neutron data the least-squares structure refinements were carried to convergence; every parameter shift in the last cycle(s) was less than one-half the standard deviation in that parameter. Thus, we actually do have a direct crystal structure refinement for human tooth enamel -- two of them, in fact, one with x-ray data and an independent one with neutron data.

As anticipated, the crystal structure of TE is similar to that of OHAp in the placement of the principal ions (Table 1). Let us compare the X-4 results with single crystal values in Table 1. Most positional parameters agree well, but there are some apparent differences which might be significant on the basis of the standard deviations obtained. These occur in the x-ray results for the $O(3)$ x, y, and z parameters; in the y parameter of P, and possibly in the x of Ca(2). Since some substitution of CO_3 for PO_4 is expected (5) and not accommodated in the models used, some distortion of the apparent

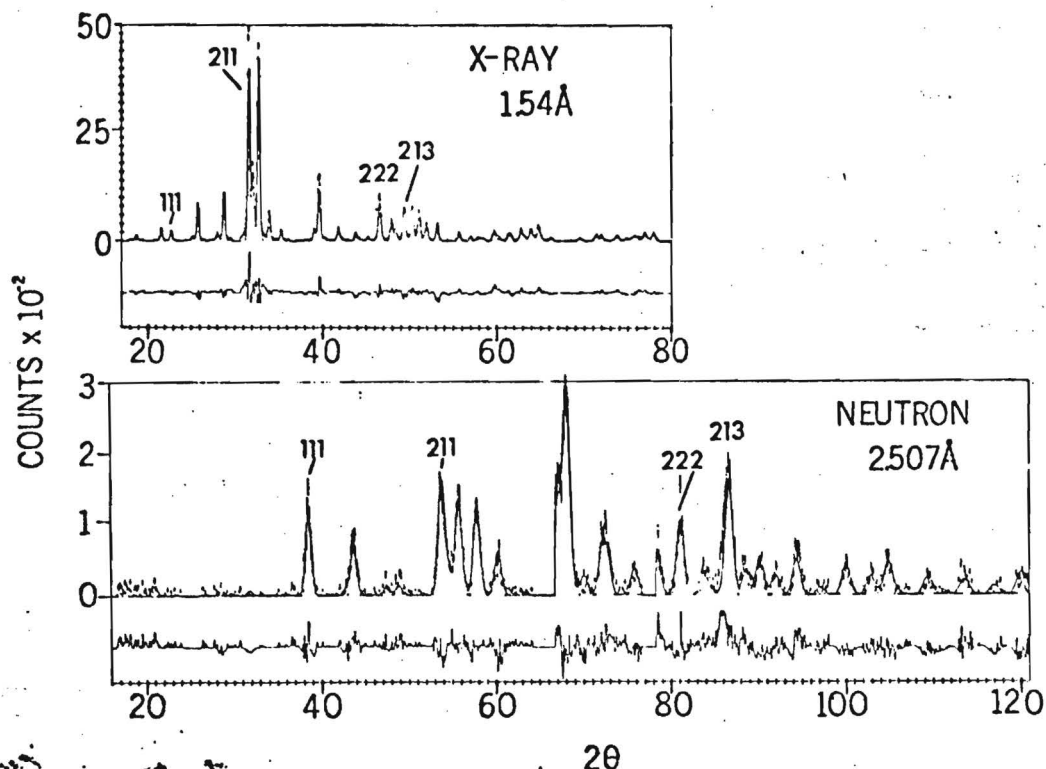


FIG. 3

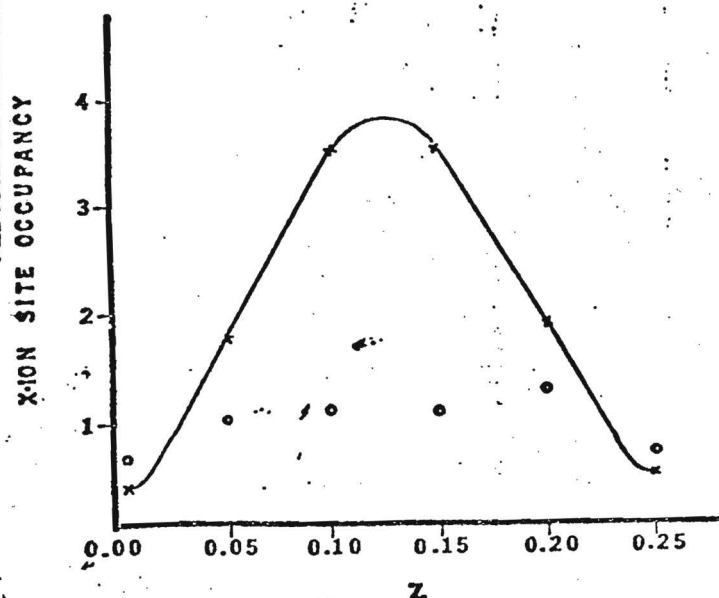
Powder diffraction patterns of TE as obtained with (a) x-rays and (b) neutrons. Observed patterns are shown by crosses, those calculated by a solid line, and the difference by the solid line patterns below the main patterns.

positions of P and O could be a consequence. Similarly, since O(3) borders the X-ion channel in which there are entities present that are neither in the model nor in OHAP (e.g., probably H_2O , a small part of the CO_3 , etc), it would not be surprising to find O(3) shifted with respect to its OHAP position. It should also be borne in mind that the atom temperature factors were not adjusted but were fixed at their single crystal values. Thus any variability of atom position caused by nearby substitutions or vacancies, which would tend to be accommodated with an increased temperature factor, would here cause a decrease of the site occupancy factor. But these "explanations", while plausible, can not be accepted as definitive for at least two reasons, as follows.

First, the standard deviations in the X-4 and other X refinements are smaller than is realistic for comparing structures. The proof of this statement lies in the differences obtained for these same (and other) positional parameters in the x-ray refinements with the different models. For X-1 through X-4 the data are the same, the program used and the manner of its use are the same, and the models differ only in the X-ion region. Yet positional parameters of other ions, including ones not nearby, such as P and O(1), are affected by much more than the indicated standard deviations. Since even the model for X-4 is incomplete, then the possibility is open that further improvements in the model could result in further parameter shifts much larger than the indicated standard deviations. Further, several additional refinement runs (not otherwise reported here) showed that the site occupancies and even the

FIG. 4

X-ion site occupancies obtained from models 3 and 4. O= neutron data; X= x-ray data.



position parameters of O(1) and O(2), for example, could converge to either of two general values depending on the starting values used. (Initial misplacement of O(1) by 0.8\AA led to a "refined" value differing from the one here by 0.7\AA with only a less than 2% difference in R_{wp}). It is believed that this phenomenon may be a consequence of (i) not having in the model CO_3 substituting for PO_4 , and (ii) a probable tendency of the Rietveld method to be more troubled by false minima than are single crystal refinements. In any event, it is a warning against over interpretation of these initial results.

Second, the neutron and x-ray results often differ from the single crystal results in opposite ways, especially for O(3) (cf N-4 and X-4 Table 1). Since the relative scattering powers of the atoms do differ according to whether x-rays or neutrons are being scattered, one could argue that these positional parameter differences may simply reflect the differing scattering consequences of partial substitutions at or near the affected atom sites. But, at this stage, there is no analysis in hand to support or deny such possibilities. Firm conclusions about possible significance of the positional parameter differences must therefore be held in abeyance.

As Table 1 shows, the detailed results are model dependent, even for atoms not adjacent to the region in which the models differ. Although the R_{wp} factors suggest that models 3 and 4 are best for the x-ray case and 4 and 5 for the neutron case, the differences in R_{wp} 's are only small differences in large quantities. [The Hamilton R-ratio test (13) of significance of differences in R's can not readily be applied to R_{wp} because of ambiguity about the number of independent observations. It could be applied to R_B , but R_B is an inferior indicator.] It is useful, then, to see which refinements lead to

Table 1†

		X-1*	N-1	X-2	N-2	X-3	N-3	X-4	N-4	N-5	Single Crystal S & Y
Ca(1)	z	007(1)	-024(2)	005(1)	-023(2)	003(1)	-023(3)	003(1)	-023(3)	-024(3)	002
	n**	238(2)	387(9)	237(2)	381(10)	239(2)	350(4)	239(2)	354(12)	343(10)	
Ca(2)	x	250(0)	243(2)	251(0)	247(2)	250(0)	253(2)	250(0)	253(2)	253(2)	247
	y	992(0)	988(3)	992(0)	991(2)	994(1)	993(2)	994(1)	997(2)	1000(2)	993
	n	375(2)	500-	374(2)	500-	389(2)	500-	389(2)	500-	500-	
P	x	400(1)	395(4)	400(1)	402(3)	402(1)	406(4)	402(1)	407(4)	407(4)	399
	y	352(1)	364(3)	354(1)	368(3)	359(1)	374(3)	359(1)	374(3)	375(3)	369
	n	383(3)	326(13)	382(3)	341(14)	413(3)	366(15)	412(3)	365(15)	367(15)	
O(1)	x	317(1)	322(2)	317(1)	322(2)	332(1)	323(2)	332(1)	323(2)	323(2)	328
	y	474(1)	476(2)	475(1)	476(2)	484(2)	478(2)	484(2)	478(2)	477(2)	485
	n	294(5)	500(13)	288(5)	516(13)	257(6)	524(14)	257(6)	527(14)	525(13)	
O(2)	x	595(1)	574(3)	595(1)	576(3)	589(1)	574(3)	589(1)	574(3)	574(3)	587
	y	465(1)	457(2)	463(1)	458(2)	460(1)	459(2)	460(1)	459(2)	459(2)	465
	n	375(6)	400(11)	374(6)	407(12)	470(6)	419(16)	469(1)	420(14)	414(14)	
O(3)	x	354(1)	329(1)	355(1)	331(1)	364(1)	333(1)	364(1)	333(1)	333(1)	344
	y	271(1)	249(1)	271(1)	249(1)	277(0)	248(1)	277(1)	243(1)	247(1)	258
	z	048(1)	066(1)	051(1)	067(1)	054(1)	067(1)	054(1)	067(1)	067(1)	070
	n	1000—	920(16)	1000—	955(17)	1000—	991(16)	1000—	990(16)	994(16)	
O(H)	z	134(1)	149(4)	195 -	198 -					198 -	196
	n	288(4)	170(8)	113(3)	077(8)					142(7)	
Cl	z	—	—	400-	390-					444-	
	n	—	—	089(2)	068(7)					079(5)	
n(O _H)	z=0.00					028(6)	053(18)				
	z=0.05							162(4)	093(14)		
	z=0.10					342(10)	094(29)				
	z=0.15							345(10)	096(23)		
	z=0.20					172(4)	116(13)				
	z=-.25							034(6)	098(14)		
	R _{wp} (%)	27.1	27.0	27.4	26.7	25.51	26.7	25.51	26.7	26.8	
	R _p (%)	24.4	29.9	24.3	29.7	22.51	29.7	22.51	29.7	29.7	
	R _B (%)	—	36.1	—	36.7	—	37.6	—	37.6	37.9	
Overall B		4.2(2)	5.6(3)	4.1(2)	5.3(3)	3.2(2)	4.9(3)	3.2(2)	4.9(3)	5.0(3)	
	a (Å)	9.441(2)	9.447(2)	9.441(2)	9.447(2)	9.442(2)	9.447(2)	9.442(2)	9.447(2)	9.447(2)	
	c (Å)	6.877(1)	6.892(2)	6.877(1)	6.892(2)	6.877(1)	6.892(2)	6.877(1)	6.892(2)	6.891(2)	
Zero pt		-0.119	0.294	-0.120	0.293	-0.118	0.294	-0.118	0.294	0.294	

† All position and site occupancy factors have been multiplied by 10³.

* All X (for X-ray) refinements used PS349 data.

N stands for refinements with neutron data.

** n = site occupancy factor = site occupancy/site multiplicity created by symmetry.

TABLE 2
P-O Distances

<u>Bond</u>	<u>Refinements*</u>	<u>Distances</u> ^o (Å)
P-O(1)	X-1	1.69(3)
	X-3	1.62(3)
	SX	1.54(<1)
	N-2	1.54(7)
	N-3	1.53(8)
P-O(2)	X-1	1.60(2)
	X-3	1.53(2)
	SX	1.54(<1)
	N-2	1.42(7)
	N-3	1.37(8)
P-O(3)	X-1	1.54(2)
	X-3	1.59(2)
	SX	1.53(<1)
	N-2	1.59(5)
	N-3	1.63(6)

*SX= From OHAp single crystal results of Sudarsanan & Young (14).

the most reasonable stereochemical results, such as the P-O distances in the PO₄ group. Table 2 gives representative results. On this basis it appears that refinements X-3 & X-4 are best (and equally good) for the x-ray case and N-2 is slightly the best for the neutron case, although it seems to have a problem with the P-O(2) distance.

Reasonable results suggestive of new information have been obtained for the distribution of scattering density along the 6₃ axis. The axial site occupancies obtained in refinements X-3, X-4, N-3 and N-4 (Table 1) are plotted in Fig. 4. Fortunately, the separate results from the two models do seem to be consistent within either the x-ray case or the neutron case. Thus the plots probably are at least qualitative representations of the distributions along the X-ion channel of the scattering densities for x-rays (X) and for neutrons (O). It is clear, from the x-ray plot, why the x-ray attempts to refine the z parameters of two atoms placed initially at $\underline{z} = 0.19$ and $\underline{z} = 0.44$ (equivalent to 0.06) resulted in the two atoms moving onto each other -- there is a single maximum in the density and it is between those two starting positions.

The differences between the scattering densities sensed by the two radiations can be utilized for additional analysis based on the differing scattering powers of various atoms for x-rays vs neutrons. The scattering powers of H and of D are -0.38×10^{-12} cm and $+0.65 \times 10^{-12}$ cm, respectively, for thermal neutrons but are essentially identical for x-rays. The neutron result in Fig. 4 is rather like what one would expect from partially deuterated OHAp (as was the TE used for the neutron data) wherein O(OH) occurs at $\underline{z} \approx 0.20$ and D at $\underline{z} \approx 0.06$. The magnitude of the site occupancy (neutron) at $\underline{z} \approx 0.20$ is even consistent with the previously noted OH deficiency in TE (2, 19). Infra-red spectroscopy showed that the TE was not fully deuterated, but only about 50% (Fig. 2). Thus some H would also be expected at $\underline{z} = 0.06$. Further, the little Cl known to be present (~ 1 Cl in every 5-10 cells) would be very near, at $\underline{z} = 0.06$ to 0.11. H has a negative scattering length (-0.38×10^{-12} cm vs 0.65×10^{-12} cm for D) so its presence would diminish the height of the peak. Cl has a positive scattering length (0.95×10^{-12} cm), so its presence as a substituent for OH would increase the peak at $\underline{z} = 0.06$ relative to that at $\underline{z} = 0.20$. If Cl is substituting for 1/20 of the OH's one can calculate that, if the TE is only one-half deuterated at the OH sites, the ratio of scattering density at 0.20 to that at 0.06 would be 0.88, approximately what is shown in Fig. 4.

The differences between the distributions indicated by x-rays and by neutrons may be more interesting. A substantial amount of H in the mid region around $z = 0.10 - 0.15$ would decrease the positive density "seen" by neutrons but would increase it only slightly for x-rays. A source of a much bigger increase in the x-ray scattering density in this region is needed to explain Fig. 4. The 2-4 wt% H_2O present (20) is present as "caged" water (21), i.e., not rigidly held but not quite freely tumbling. If these H_2O molecules are in fact present in the 6_3 axis region (although, note that Dibdin's work (22) suggests that they may not be so structurally incorporated) in more or less random orientation, the centers of the distributions of their O ions and of their H ions would coincide. The 2 H's have total scattering length for neutrons of $-0.76 \times 10^{-12} \text{ cm}$ and the O has $0.58 \times 10^{-12} \text{ cm}$. Thus H_2O in random orientation would scatter neutrons much as a very large ion with a somewhat negative (and angle dependent) scattering factor. Such a model with the centers of the H_2O distributions placed at $z \approx 0.12 - 0.14$ could reconcile the very different appearances of the x-ray and neutron scattering density distributions in Fig. 4 while also providing some account of the substantial amount of H_2O known to be present. Even the magnitude of the occupancy factor at the presumed H_2O "site" is about right, implying about 2 molecules of H_2O per unit cell corresponding to 3.6 wt%, a value in the observed range. Like refinement of x-ray data from a similar, though possibly not identical, TE specimen resulted, however, in site occupancies only about one half as large. Thus some caution in interpretation is still required.

Possibly the fact that the H_2O is not freely tumbling means that the orientation is not entirely random. Some preferred orientation of the H_2O molecule could be accommodated in this model - in fact might be wanted - but it would be a preferred orientation with the H's (of the H_2O molecule) tending to be off the 6_3 axis more than along it. We know of no NMR, i.r., chemical or other data which would preclude this model for the H_2O , but neither do we know of any which confirm it. What we have established with the present results is plausibility, not proof.

Because neutrons and x-rays are scattered somewhat differently by atoms, and since the model used does not incorporate all entities and substitutions present, some differences between x-ray and neutron results should be expected for off-axis atoms, as well, especially for site occupancy factors.

One of the expected differences between TE and OHAp is a calcium deficiency ($Ca/P \approx 1.58$ in TE instead of 1.67 in OHAp, see compilation by Young (7)). The x-ray results (Table 1) show a deficiency of both $Ca(1)$ & $Ca(2)$ compared to $O(3)$ but the neutron results do not. Whether this difference arises from the negatively scattering H in the acid phosphate (HPO_4) present in TE (5 wt% reported by Arends and Davidson (23)), but not included in the refinement model, is not yet known.

It is known from chemical balance studies (24,25) that some phosphate can be replaced by CO_3 in apatite. From i.r. studies it is known that (i) the plane of the CO_3 molecule is inclined to the c axis (26) and (ii) <90% of the CO_3 structurally incorporated in TE ($\sim 2.8 \text{ wt\%}$ or roughly one CO_3 per two unit cells) is in this site, somehow replacing PO_4 . A much proposed model is that of CO_3 substituting on the "slant face" of the PO_4 , i.e., involving O ions near the $O(1)$ and the $O(2)$ and one of the two $O(3)$'s. Such a substitution would have the effect of decreasing the measured site occupancy for $O(3)$ relative to $O(1)$ and $O(2)$ by about 2%. Both x-ray and neutron results (X-4 & N-2) agree that this does not seem to occur or that, if it does, it is masked by a much stronger opposite effect.

Discussion

In view of the newness of the x-ray analysis techniques used (27) and the as-yet unexplained discrepancies between x-ray and neutron results, it is gratifying that reasonably definitive results have been obtained for the locations of the principal atoms and, especially, the indications of the probable location of structurally incorporated water. Although it has not been possible at this time to produce similarly definitive results about other "substitutions" such as CO_3 and the acid-phosphate H ion site, for example, the preceding two paragraphs do indicate some of the kinds of analyses and interpretations that will become possible after much further study with the Rietveld method.

Although the refinement process has been carried as far as it can be with each of these data sets and with the model (crystal structural and reflection profile) and (rather extensive) computer programs used, and some new results have been obtained, unexplained discrepancies still remain. Clearly, there are some artifacts yet to be understood, and there is much more of the structural detail of TE yet to be determined with further work. The two main ways in which the present refinements are incomplete are (i) absence from the model of other entities known to be present in the TE crystal structure, especially CO_3 , HPO_4 , and H_2O and (ii) the actual individual reflection profiles in the x-ray case are not well fit by the Gaussian form used (nor by Lorentzian); a more complex function is needed (28).

R_{wp} values for Rietveld refinement with x-ray data often turn out to be about double those with neutron data because the reflection profile function used better fits reality in the neutron case (29). The fact that the R_{wp} values obtained here for the neutron case are much more than one half of those for the x-ray case, and both are large, suggests that the principal improvement needed is in the structural model used, i.e., the inclusion in it of other entities known to be present but not yet located. Thus, one can predict that further work with improved models and additional data, including data for TE changed by various treatments, will be fruitful in delineating differences in structural detail between TE and OHAp. Only then can we expect to understand fully the role that entities such as CO_3 , Cl and H_2O play in determining the properties of human tooth enamel. This first crystal structure refinement of TE is a step in that direction.

Acknowledgements

We thank Dennis B. Wiles for the utilization of his new computer program and James Cagle for collecting the neutron data. This work has been supported by the USPHS through NIDR Grants DE-01912 and DE-04151.

References

1. A.S. Posner, C. Fabry and M.J. Dallemagne, *Biochim. et Biophys. Acta* 15, 304 (1954).
2. R.A. Young and S. Spooner, *Archs. oral Biol.* 15, 47 (1969).
3. R.Z. LeGeros, O.R. Trautz, J.P. LeGeros and E. Klein, "Pyrolysis of Biological Apatites: X-ray Diffraction and Infrared Studies", paper 177, 48th General meeting of the IADR, New York, NY (1970).
4. R.A. Young, D.W. Holcomb and P.E. Mackie, *J. Dent. Res.* 56, B223 (1977).
5. R.Z. LeGeros, J.P. LeGeros, O.R. Trautz and E. Klein, *Dev. Appl. Spectrosc.*, 7B, 3 (1970).
6. R.A. Young and D.W. Holcomb, *J. Dent. Res.* 55, B255 (1976).
7. R.A. Young, *Clinical Orthopaedics* 113, 249 (1975).
8. H.M. Rietveld, *J. Appl. Cryst.* 2, 65 (1969).
9. R.A. Young, P.E. Mackie and R.B. Von Dreele, *J. Appl. Cryst.* 10, 262 (1977).
10. D.B. Wiles and R.A. Young, *Amer. Cryst. Assoc. Program & Abstracts, Series 2*, 7, 56 (1979).
11. *International Tables for X-ray Crystallography*, IV, 99. The Kynoch Press, England (1974).
12. *International Tables for X-ray Crystallography*, IV, 148. The Kynoch Press, England (1974).
13. G.E. Bacon, *Neutron Diffraction*, 2nd ed. p. 31, University Press, Oxford (1962).
14. K. Sudarsanan and R.A. Young, *Acta Cryst.* B25, 1534 (1969).
15. R.A. Young, K. Sudarsanan and P.E. Mackie, *Extrait du Bulletin de la Société Chimique de France*, (n° special), 1760 (1968).
16. G. Montel, *Extrait de Bulletin de la Société Chimique de France* (n° special), 1693 (1967).
17. K. Sudarsanan and R.A. Young, *Acta Cryst.* B34, 1401 (1978).
18. W.C. Hamilton, *Acta Cryst.* 18, 502 (1965).
19. M.L. Bartlett and R.A. Young, "Structural OH Deficiency in Tooth Enamel and Hydroxyapatite", paper 125, 50th General meeting of the IADR, Las Vegas, Nevada (1972).
20. M.F. Little and F.S. Casciani, *Archs. oral Biol.* 11, 565 (1966).
21. H.M. Myers, *Nature* 206, 713 (1965).

22. G.H. Didbin, Archs. oral Biol. 17, 433 (1972).
23. J. Arends and C.L. Davidson, Calcif. Tiss. Res. 18, 65 (1975).
24. D. McConnell, Bull. Soc. Franc. Min. Crist. 75, 428 (1952).
25. G.H. McClellan and J.R. Lehr, Am. Mineral. 54, 1374 (1969).
26. J.C. Elliott, The Crystallographic Structure of Dental Enamel and Related Apatites, Ph.D Thesis, University of London (1964).
27. P.E. Mackie and R.A. Young, Acta Cryst. A31, S198 (1975).
28. R.A. Young, P.E. Mackie and D.B. Wiles, Acta Physica Polonica (in press).
29. M.I. Kay, R.A. Young and A.S. Posner, Nature 204, 1050 (1964).

Mackie, Paul E.
209-32-0029

Interim Progress Report

A. INTRODUCTION

A1. Objective:

The long-range goal of this work is to obtain an understanding of the occurrence, location, binding, variety, changeability and functional role of the "water" in tooth enamel in relation to various properties of human teeth

A2. Background

It is well established that water is present in tooth enamel (TE) as a significant constituent. Various investigators (Myers, 1965; Myers and Myrberg, 1956; Myrberg, 1968; Little and Casciani, 1966; Casciani, 1971; Dibdin, 1972) have reported water to be present in amounts of 2 to 7 wt%. Many investigators, recognizing its possibly important biophysical and biochemical role in caries attack and tooth properties, have studied "water" in tooth enamel. However, the location(s) and role(s) of water are still a subject of controversy. One point of particular interest is the occurrence of any irreversible processes in the enamel as a result of preparative techniques such as drilling and the accompanying localized dehydration due to high temperatures generated. Such irreversible processes would be taking place at the very surface which must interface with restorative materials.

Many varied techniques have been used to study water in tooth enamel. Burnett and Zenewits (1958) measured the weight changes in whole teeth and dentin resulting from heating them at various temperatures from 61 to 197°C under both vacuum and normal atmospheric conditions. They found that the dental moisture depended upon the heating temperature and atmospheric pressure. They also investigated the rehydration of dental enamel at various temperatures and relative humidities and found the moisture could be only partially restored. Burnett (1958) also suggested that the moisture content of enamel did not decrease with age as it does in bone. However, Toto (Toto, et al., 1971) found less "water" in old teeth than young teeth. Gwinnett (1966) performed quantitative polarized light studies of enamel and found the pore volume of "normal enamel" (non-cariou) to be 0.2%. He interpreted the moisture absorption properties of normal enamel as being due to a type of molecular sieve. Dibdin's (1969) krypton absorption studies demonstrated an easily accessible pore system in enamel measuring 10 to 300Å with a volume of 0.26%. Both of these measures of pore volume in enamel are low compared to the volume of free water found in enamel, 1 - 2% (Burnett and Zenewitz, 1958). Moreno and Zahradnik (1973) have investigated the pore structure of dental enamel with the water-vapor sorption-isotherm technique. They found considerable hysteresis in the sorption isotherm indicative of a pore system in enamel dominated by constrictions. Moreno and Zahradnik found the distribution of pore radii to be bimodal, the peaks in the distribution corresponding to pores with radii of 23 and 58Å (if cylindrically shaped pores are assumed). They found labile water in the range of 1.8 to 3.6% by volume. Thus, the accessible pore volume of enamel seems to be 10 times greater with water than with krypton.

Although the question of the amount and, in particular, the location and state of binding of water in tooth enamel (TE) have been the subject of many investigations, there has not been general agreement among the various investigators regarding the results. Little and Casciani (1966) suggested, on the basis of NMR evidence, a loosely bound (D_2O exchangeable) water present at ~0.6 to 1wt% and two forms of caged but freely tumbling water. One form of the caged water

was associated with the variable Ca/P ratio and was found to be removable by heating at 900°C. They found the same rather narrow (for a solid) NMR line width (50mG) for all of the protons and thus inferred the absence of tightly bound protons (e.g., structural OH). They suggested that the second form of caged water, found to be removable only between 900 and 1300°C, was water located at the sites normally assigned to OH⁻ in hydroxyapatite and, thus, they speculated that apatite in tooth enamel might be a hydroapatite rather than hydroxyapatite. Young and Spooner (1969) have shown from neutron diffraction and deuteration experiments that as much as 30% of the structural hydroxyls in TE are missing. O'Shea and Weaver (1974) showed from laser Raman spectroscopy that TE had 30% less structural OH than in synthetic hydroxyapatite. More recently Young (1977) reports that TE deuterates at least as rapidly as the unheated aqueous preparations of hydroxyapatite and in TE, in particular, the heating decreases the "broad water" band in the i.r. spectrum and increases the structural OH⁻ band at 3572cm⁻¹.

Dibdin (1972) found that the "narrow-resonance" (i.r., in NMR spectra) protons of enamel are easily removed at room temperatures by lowering the humidity and all that remains is a broad (1G) resonance line which can be explained by 1.6 - 2 wt% strongly bound water or 3 - 3.8 wt% hydroxyl ions. A realistic model is probably a combination of strongly bound water with an accompanying hydroxyl ion deficiency. It has been suggested (Dibdin, 1972) that the discrepancy in the temperature stability of the narrow proton resonance can, in part, be explained by the readsorption of atmospheric moisture during the transfer from the drying container to sealed NMR sample tubes. Dielectric measurements of apatites, which are very sensitive to the presence of water, in vacuo and in air indicated (Rausch, 1976) that atmospheric moisture is readsorbed very rapidly under ambient conditions for pressure, temperature and humidity. The process is essentially completed in less than 10 minutes. Most of the experiments to date (with the exception of Dibdin, 1972) appear to have lacked rigid control results of kinetics studies of D₂O exchange, weight loss experiments, i.r. and NMR spectroscopy can all be adversely affected by uncontrolled moisture readsorption.

There is evidence from several different techniques that water is incorporated in the apatite structure of human tooth enamel. Bartlett and Young (1972) used quantitative IR to observe water in samples of enamel which had undergone various heating schedules and found some apparent correlation of changes in amounts of water with both changes in lattice parameters and reduction of structural OH deficiency. Similarly, O'Shea, Bartlett and Young (1972) observed similar changes with laser-Raman spectra. Furthermore, the electron spin resonance studies of Peckauskas and Pullman (1974) indicated the presence of tightly bound water in synthetic apatite. LeGeros et al., (1970) correlated weight loss after heating to 400°C with an a axis contraction; but found the weight loss after heating to 200°C was not associated with lattice contraction. In more recent work, LeGeros et al., (1977) found the weight loss below 200°C to be reversible, while the weight loss between 300°C to 400°C to irreversible and correlated with a axis contraction. Recent work by Arends and Davidson (1975) and Davidson and Arends (1976) attribute part of the weight loss in the 150°C to 400°C range to water resulting from reactions of HPO₄ ions with structural OH. They show (by IR) that sound enamel contains approximately 6 wt% HPO₄.

References

- Arends, J. and Davidson, C.L. (1975) Calcif. Tiss. Res., 18, 65.
- Bartlett, M.L. and Young, R.A. (1972) IADR Meeting, Las Vegas, Nevada, Paper 125.
- Burnett, G.W. and Zenewitz, J. (1958) J. Dent. Res., 35, 581.
- Casciani, F.S. (1971) Tooth Enamel II (edited by Fearnhead, R.W. and Stack, M.V.) John Wright and Sons Ltd. Bristol, pp. 14-23.
- Davidson, C.L. and Arends, J. (1976) IADR Meeting, Miami, Florida, Paper 771.
- Dibdin, G.H. (1969) J. Dent. Res., 48, 771.
- Dibdin, G.H. (1972) Arch. oral Biol., 17, 433.
- Gwinnett, A.J. (1966) J. Dent. Res., 45, 120.
- Hewat, A.W. (1973) AERE Report R7350. The Rietveld Computer Program for the Profile Refinement of Neutron Diffraction Powder Patterns Modified for Anisotropic Thermal Vibrations.
- LeGeros, R.Z., Trautz, O.R., LeGeros, J.P. and Klein, E. (1970) IADR Meeting, New York, Paper 177.
- LeGeros, R.Z., Quiroigico, G., Bone], G., LeGeros, R., (1977) IADR Meeting, Copenhagen, Paper 48.
- Little, M.F. and Casciani, F.S. (1966) Archs. oral Biol., 11, 565.
- Moreno, E.C. and Zahradnik, R.T. (1973) Archs. oral Biol., 18, 1063.
- Myers, H.M. (1965) Nature, Lond., 206, 713.
- Myers, H.M. and Myrberg, N. (1965) Acta odont. scand., 23, 593.
- Myrberg, N. (1968) Trans Roy. Sch. Dent. Stockholm and Umea, 14, 1.
- O'Shea, D.C., Bartlett, M.L. and Young, R.A. (1972) IADR Meeting, Las Vegas, Nevada, Paper 472.
- O'Shea, D.C., Weaver, D.P. (1974) IADR Meeting, Atlanta, Georgia, Paper 238.
- Peckauskas, R.A. and Pullman, I. (1974) IADR Meeting, Atlanta, Georgia, Paper 239.
- Poole, D.F.G. (1971) Tooth Enamel II (edited by Fearnhead, R.W. and Stack, M.V.) John Wright and Sons Ltd., Bristol, pp. 43-46.
- Rapp, G.W. (1971) J. Dent. Res., 50, 1284.
- Rausch, E.O. (1976) Ph.D. Dissertation, "Dielectric Properties of Chlorapatite", Georgia Institute of Technology, Atlanta, Georgia.
- Rietveld, H.M. (1969) J. Appl. Cryst., 2, 65.

References (continued)

- Scott, D.B., Simmelink, J.W. and Nygaard, V. (1974) J. Dent. Res., 53, 165.
- Soni, N. and Brudevold, F.A. (1959) J. Dent. Res., 38, 1181.
- Von Dreele, R.B. and Cheetham, A.K. (1974) Proc. Roy. Soc. A 338, 311.
- Young, R.A. (1977) Application for Continuation Grant, NIDR, DE 01912-14.
- Young, R.A. and Spooner, S. (1969) Archs. oral Biol., 15, 47.

A4. Comprehensive Progress Report:

A4a) Covering the period (1 June 1975 to 16 May 1977)*

A4b) Summary

During this initial grant period (DE04151-01, 02, and 03), the work on understanding the occurrence, location, binding, variety, changeability and functional role of "water" present in human dental enamel progressed along six fronts. Major project activities were in the areas of: (i) acquisition of human teeth and the preparation of enamel powders, (ii) x-ray diffraction study (XRD) of powdered human tooth enamel, in vacuum, from 25°C to 500°C, (iii) thermogravimetric analysis (TGA) of a number of different enamel samples with different ages and particle sizes, (iv) infra-red analysis (i.r.) and dynamic evolved gas infra-red (DGIR) analysis of pyrolyzed enamel and the evolved products of pyrolyzed enamel respectively, (v) mass spectrometry (MS) of the gaseous products of pyrolyzed human tooth enamel, (vi) equipment design, fabrication and modification for the XRD, MS, TGA and DGIR experiments.

A major accomplishment during this report period was the substantial step forward in the direct study of human tooth enamel itself by the Pattern-Fitting-Structure-Refinement method (PFSR). This method, PFSR, applied to powdered human tooth enamel has provided for the first time quantitative structure analysis of the crystalline portion of tooth enamel, per se.

A4c) Detailed Report

Sample Acquisition and Preparation

The collection and preparation (see Method of Procedure for details of the preparation techniques) of whole sound human teeth, both age differentiated and pooled, has been a continuous activity during the first grant period. Approximately 2, 50, and 50 grams of TE powder have been prepared for the under 15 years, 16-50 years, and the 51 and over categories, respectively. Another 100 grams of enamel powder have been prepared from teeth with no age differentiation. These figures includes both the heavy (sp. g. >2.95) and medium (2.95 > sp. g. > 2.84) density fraction. A backlog of about 200 whole teeth exists on which no work has been done yet.

X-ray Diffraction & PFSR of Human Tooth Enamel (TE)

A powder x-ray diffraction environmental chamber was designed and built. This chamber is capable of heating the sample to 500°C while maintaining, the sample under a vacuum of 20 μ (see Photos 1 through 3). The design is such that gases evolved from the sample as it is pyrolyzed may be collected in an external glass vessel for further analyses (e.g., mass spectrometry). This chamber will also be used to maintain the sample in controlled atmospheres (e.g., various humidities, N₂ or CO₂).

*See Changes in Effort of the Summary Progress Report of the first project year. That section explains that full-time effort was delayed until January 1976. In addition, a 1/3 reduction in effort was required by the reductions made by Council in the personnel services of originally submitted budget.

This chamber has been used to collect 14 x-ray diffraction data sets on a "pooled" enamel sample at 8 different temperatures from room temperatures to 500°C and then back to room temperature under vacuum (~ 20 milliTorr) conditions. These 14 data sets have been analysed by the method of Pattern-Fitting-Structure Refinement (PFSR). Since PFSR is a relatively new technique (see "Application of the Pattern-Fitting-Structure-Refinement Method to X-ray Powder Diffractometer Patterns", R.A. Young, P.E. Mackie and R.B. Von Dreele, Journal of Applied Crystallography, (1977)) a short description is warranted at this point.

The method of PFSR entails using a computer program in conjunction with an atomic-scale model of the material under study to calculate an x-ray powder diffraction pattern. The atomic-scale model is defined by specifying where each atom is located (i.e., what are the x, y and z's of each atom) specifying how each atom is moving and by specifying the probabilities with which one would find a given crystallographically unique atom in a given unit cell. In addition to specifying parameters which describe the atomic model, one must specify other parameters which describe the "state" of the sample (e.g., crystallite size, strain, preferred orientation, etc.) and which describe the experimental setup (e.g., incident wavelengths or spectral distribution, instrumental resolution and aberrations). After everything is specified an x-ray powder diffraction pattern can be calculated. In practice, this calculated pattern will differ from the observed pattern. The parameters of the model (and experiment!) must then be adjusted or changed to make the calculated pattern fit the observed pattern better in a least-squares sense. In this manner (with a method quite similar to that used for single-crystal x-ray analyses) one can obtain directly crystal structure details of human tooth enamel. In practice, many cycles of refinement and much computer time are needed to gradually refine the atomic model (e.g., adding missing constituents of the model such as impurities, until the desired degree of fit is obtained).

The PFSR analyses of the 14 data sets described above have not been fully completed yet, but are far enough along so that some significant questions are answered, while still other questions were raised which have suggested additional experiments to be performed. So far, the positions and site occupancies of the calciums (Ca(1) and Ca(2)) and the atoms in the phosphate group (P, O(1), O(2) & O(3)) have been determined (see Table I). While there is evidence of significant changes in atomic details occurring along the hexad axis of the apatite-like structure as a function of temperature, results of the present refinements can not be interpreted conclusively for the atoms on this axis.

From Table I and Figure I one can see that the most obvious difference in structural parameters between TE and Holly Springs hydroxapatite is a rotation of the PO_4 groups about a axis which passes through the O_3 's. There is a slight increase in the size of the Ca_2 and O_3 triangles. The O_3 -P- O_3 angle is smaller in TE than in Holly Springs OHAp. Smaller-than-normal site occupancy factors for O_1 , O_2 and P relative to O_3 , suggests that there may be considerable disorder, in TE, of the PO_4 groups about the axis through the O_3 's perpendicular to the mirror planes. This hypothesis is further supported by additional PFSR refinements (incomplete at this time) with isotropic temperature factors for the calciums and PO_4 groups allowed to vary, which reveal close-to-normal temperature factors for the O_3 and P but very much enlarged thermal factors for the O_1 and O_2 .

		O ₁			
		x	y	z	s
TE	25°C	4073 _{2 5}	5222 _{3 7}	$\frac{1}{4}$.50 ₂
	185°C	4086 _{2 6}	5275 _{3 3}	$\frac{1}{4}$.41 ₂
	250°C	4058 _{2 6}	5266 _{3 2}	$\frac{1}{4}$.39 ₂
	300°C	4086 _{2 5}	5259 _{3 6}	$\frac{1}{4}$.48 ₂
	350°C	4129 _{2 5}	5321 _{3 6}	$\frac{1}{4}$.45 ₂
	400°C	4101 _{2 4}	5255 _{3 6}	$\frac{1}{4}$.49 ₂
	450°C	4109 _{2 5}	5287 _{3 7}	$\frac{1}{4}$.45 ₂
	450°C	4107 _{2 5}	5305 _{3 6}	$\frac{1}{4}$.45 ₂
	500°C	4090 _{2 7}	5243 _{4 0}	$\frac{1}{4}$.47 ₂
	500°C	4118 _{2 4}	5258 _{3 7}	$\frac{1}{4}$.46 ₂
	400°C	4104 _{2 5}	5282 _{3 7}	$\frac{1}{4}$.47 ₂
	300°C	4074 _{3 0}	5153 _{4 7}	$\frac{1}{4}$.49 ₃
	185°C	4065 _{2 4}	5232 _{3 5}	$\frac{1}{4}$.49 ₂
	25°C	4031 _{2 7}	5210 _{3 7}	$\frac{1}{4}$.44 ₂
OHAp	25°C	3282 ₂	4846 ₂	$\frac{1}{4}$	

		O ₂			
		x	y	z	s
		6633 _{4 1}	4738 _{4 3}	$\frac{1}{4}$.37 ₂
		6512 _{3 8}	4676 _{4 0}	$\frac{1}{4}$.34 ₂
		6553 _{3 6}	4729 _{3 7}	$\frac{1}{4}$.32 ₂
		6610 _{4 1}	4766 _{4 0}	$\frac{1}{4}$.34 ₂
		6603 _{3 9}	4767 _{3 9}	$\frac{1}{4}$.36 ₂
		6585 _{4 0}	4746 _{3 9}	$\frac{1}{4}$.34 ₂
		6585 _{4 1}	4716 _{4 0}	$\frac{1}{4}$.35 ₂
		6651 _{3 8}	4772 _{4 0}	$\frac{1}{4}$.37 ₂
		6559 _{4 8}	4678 _{4 8}	$\frac{1}{4}$.35 ₂
		6646 _{4 2}	4784 _{2 6}	$\frac{1}{4}$.32 ₂
		6540 _{4 5}	4669 _{4 4}	$\frac{1}{4}$.33 ₂
		6652 _{4 6}	4733 _{5 0}	$\frac{1}{4}$.42 ₃
		6608 _{4 2}	4719 _{4 1}	$\frac{1}{4}$.33 ₂
		6596 _{4 2}	4723 _{4 2}	$\frac{1}{4}$.35 ₂
		5876 ₁	4652 ₁	$\frac{1}{4}$	

		O ₃			
		x	y	z	s
TE	25°C	3448 _{2 9}	2651 _{1 9}	244 _{2 4}	1.05 ₃
	185°C	3531 _{2 3}	2697 _{1 7}	333 _{2 1}	.92 ₂
	250°C	3557 _{2 1}	2717 _{1 6}	345 _{1 9}	.90 ₂
	300°C	3427 _{3 0}	2668 _{1 9}	255 _{2 3}	.97 ₃
	350°C	3488 _{2 6}	2689 _{1 8}	283 _{2 1}	1.01 ₂
	400°C	3419 _{3 0}	2664 _{1 9}	253 _{2 3}	.96 ₂
	450°C	3471 _{2 7}	2683 _{1 8}	271 _{2 2}	.99 ₂
	450°C	3492 _{2 6}	2685 _{1 8}	278 _{2 2}	1.01 ₂
	500°C	3459 _{3 1}	2674 _{2 0}	223 _{2 6}	1.01 ₃
	500°C	3411 _{2 9}	2654 _{1 9}	249 _{2 3}	.96 ₂
	400°C	3439 _{2 9}	2657 _{1 9}	261 _{2 3}	.98 ₃
	300°C	3531 _{2 8}	2673 _{1 9}	237 _{2 6}	1.13 ₃
	185°C	3413 _{3 0}	2656 _{1 9}	249 _{2 3}	.98 ₂
	25°C	3460 _{2 7}	2657 _{1 8}	259 _{2 2}	1.01 ₂
OHAp	25°C	3433 ₁	2579 ₁	704 ₁	

		P			
		x	y	z	s
		3973 _{2 5}	3525 _{2 4}	$\frac{1}{4}$.48 ₁
		4000 _{2 0}	3586 _{2 0}	$\frac{1}{4}$.40 ₁
		4002 _{1 8}	3605 _{1 7}	$\frac{1}{4}$.40 ₁
		3953 _{2 4}	3573 _{2 3}	$\frac{1}{4}$.45 ₁
		3987 _{2 1}	3584 _{2 1}	$\frac{1}{4}$.47 ₁
		3947 _{2 4}	3563 _{2 3}	$\frac{1}{4}$.44 ₁
		3962 _{2 2}	3568 _{2 2}	$\frac{1}{4}$.46 ₁
		3993 _{2 1}	3576 _{2 1}	$\frac{1}{4}$.47 ₁
		3970 _{2 6}	3521 _{2 6}	$\frac{1}{4}$.47 ₁
		3939 _{2 4}	3549 _{2 3}	$\frac{1}{4}$.44 ₁
		3950 _{2 4}	3569 _{2 3}	$\frac{1}{4}$.46 ₁
		3984 _{2 7}	3474 _{2 7}	$\frac{1}{4}$.51 ₁
		3950 _{2 4}	3536 _{2 3}	$\frac{1}{4}$.45 ₁
		3971 _{2 2}	3532 _{2 2}	$\frac{1}{4}$.46 ₁
		3983 ₁	3683 ₁	$\frac{1}{4}$	

Table I

		Ca _I			
		x	y	z	S
TE	25°C	1/3	2/3	256 ₂₁	.350 ₆
	185°C	1/3	2/3	228 ₂₁	.290 ₅
	250°C	1/3	2/3	231 ₁₉	.288 ₅
	300°C	1/3	2/3	305 ₁₈	.356 ₅
	350°C	1/3	2/3	292 ₁₈	.352 ₅
	400°C	1/3	2/3	301 ₁₈	.352 ₅
	450°C	1/3	2/3	297 ₁₈	.343 ₅
	450°C	1/3	2/3	286 ₁₉	.341 ₅
	500°C	1/3	2/3	293 ₂₁	.343 ₆
	500°C	1/3	2/3	301 ₁₈	.342 ₅
	400°C	1/3	2/3	290 ₁₉	.345 ₆
	300°C	1/3	2/3	248 ₂₃	.357 ₇
OHAp	185°C	1/3	2/3	308 ₁₈	.347 ₅
	25°C	1/3	2/3	263 ₁₉	.338 ₅
		1/3	2/3	013 ₁	.323 ₁

Ca _{II}			
x	y	z	S
2492 ₁₁	9892 ₁₄	$\frac{1}{4}$.539 ₈
2485 ₁₀	9882 ₁₃	$\frac{1}{4}$.450 ₆
2477 ₁₀	9872 ₁₂	$\frac{1}{4}$.445 ₅
2471 ₁₁	9874 ₁₃	$\frac{1}{4}$.521 ₇
2473 ₁₀	9866 ₁₃	$\frac{1}{4}$.525 ₆
2472 ₁₀	9875 ₁₃	$\frac{1}{4}$.523 ₆
2472 ₁₀	9879 ₁₃	$\frac{1}{4}$.519 ₆
2468 ₁₀	9873 ₁₃	$\frac{1}{4}$.521 ₆
2476 ₁₂	9885 ₁₅	$\frac{1}{4}$.526 ₈
2469 ₁₀	9878 ₁₃	$\frac{1}{4}$.515 ₆
2482 ₁₀	9893 ₁₃	$\frac{1}{4}$.528 ₇
2490 ₁₂	9882 ₁₅	$\frac{1}{4}$.555 ₉
2474 ₁₁	9884 ₁₃	$\frac{1}{4}$.526 ₇
2484 ₁₀	9892 ₁₃	$\frac{1}{4}$.521 ₆
2465 ₁	9931 ₁	$\frac{1}{4}$.485 ₁

Table 1 (continued)

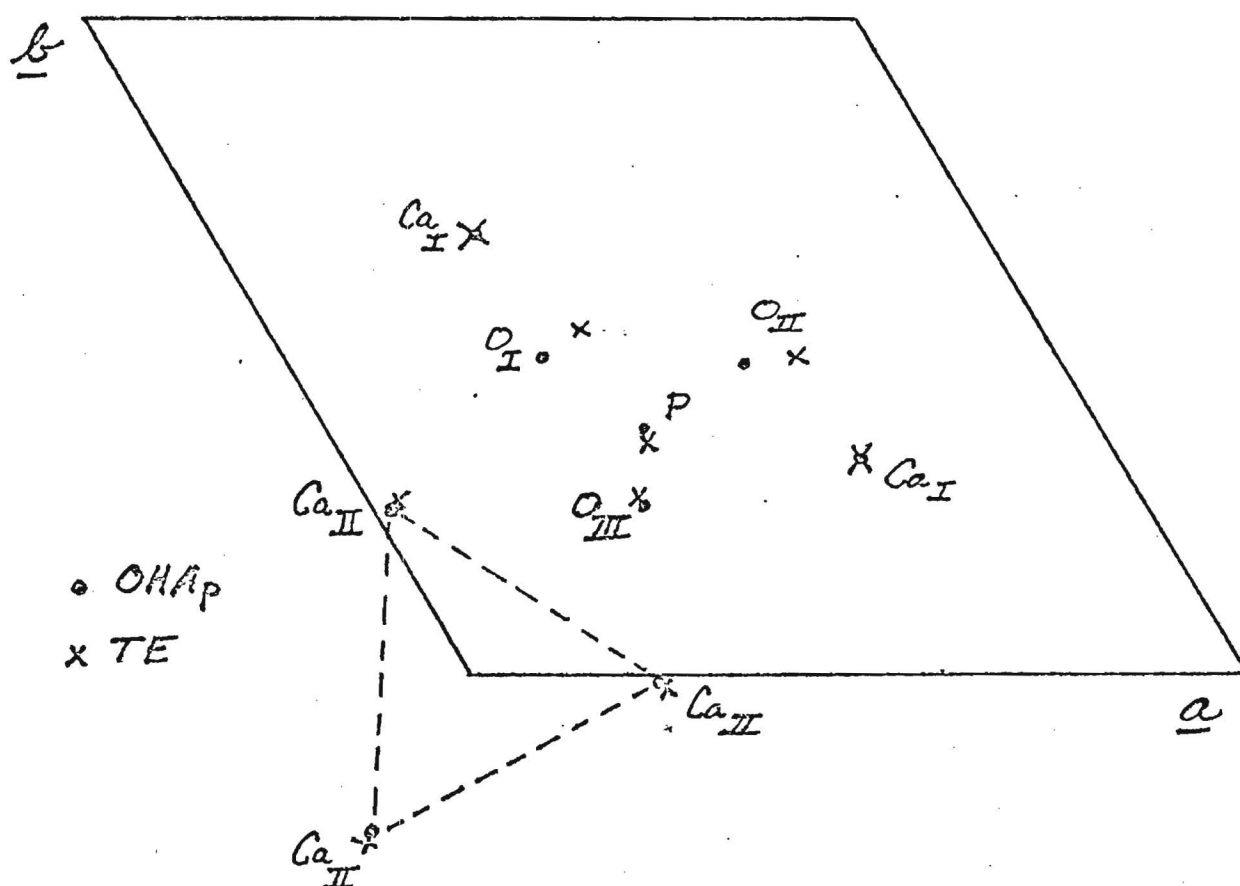


Figure 1

Lattice parameters, obtained from the PFSR refinements of the 14 data sets, show that the a parameter undergoes a decrease from $\sim 250^\circ\text{C}$ and 350°C (see Figure 2). Note that these a values are for the crystal at the indicated temperature, not after being brought back to room temperature. One question raised by these results is why the room temperature a parameter is the same before and after pyrolysis at 500°C (this appears to contradict our own previous experiences and the results of others, e.g., see R.F. LeGeros, et al. "Types of 'Water' in Synthetic and in Human Enamel Apatites", IADR, Copenhagen, 31 March-31 April, 1977). However, this experiment differed from the others in that the sample was held in a vacuum at all times during the heating regimen. Further experiments during DE04151-03 (heating the sample in vacuum and in air) should clarify this situation.

When one plots the site occupancy factors (S) for the various atoms in TE vs temperature a curious decrease in the S's is observed in the temperature range 185°C to 250°C . This coincides both with (i) the temperature at which chlorapatite is known to undergo a phase transition and (ii) the principal loss of weight as seen with TGA (primarily water). This decrease in the S's precedes ($\sim 75^\circ\text{C}$) the observed decrease in the a lattice parameter. These decreased S values could be indicating increased disorder (dynamic or static) as a precursor to the loss of material "from the lattice" indicated by the decreased a.

During our early refinements with tooth enamel data, what appeared to be a micro-crystalline ($\approx 50\text{\AA}$) calcium-phosphate phase was observed as a residual background. What first brought our attention to this, was the lack of fit (particularly in "tail" regions of the Bragg reflections) in the angular regions of 30° to 36° , 38° to 41° , 46° to 53° , and 59° to 66° ($\lambda = 1.54$). Very broad ($\approx 5^\circ$ FWHM) diffraction peaks occur in these angular regions when an observed tooth enamel diffraction pattern is convoluted with a gaussian crystallite size function of 50\AA width at half maximum. This identification is not unique to apatite though, since other calcium-phosphates (e.g., $\text{Ca}_4\text{P}_2\text{O}_9$, octa calcium-phosphates, etc.) yield similar peaks in these regions when "smeared" by the same broadening function. It will be interesting to see if this apparent micro crystalline component is present and varies with age with the age-differentiated enamel samples. The PFSR computer program is presently being completely re-written (under DE 01912-14, Professor R.A. Young, PI) to correct many of its present problems. The resolution of the possibility of a bi-modal distribution of crystallite sizes in TE awaits this new PFSR program with its improved profile functions.

Thermogravimetric Analysis (TGA) of Human TE

In the TGA work on TE, the curves exhibit "peaks" or "breaks" only as changes in slope. With large particle size there is a sharp break in the TGA curve at $\sim 410^\circ\text{C}$. With smaller particle sizes the break at 410°C is smaller. For larger particle sizes, bits of sample are actually expelled from the weighing tray as the temperature is increased. This correlates with our i.r. observations that CO_2 is rapidly evolved at 350°C . Water, while it is given off continuously as TE is heated, is rapidly evolved in the temperature range 280°C to 360°C . Apparently the CO_2 (which is released from CO_3 , as IR analyses before and after pyrolysis show reduction--eventually to zero-- of the CO_3 present in the TE specimens) and the water are unable to escape from the TE macro-structure at lower temperatures; but at higher temperatures breakdown of the TE macro-structure then releases them, sometimes explosively if the particles are large. This may relate to Dibdin's (1969) observation from BET measurements that the pore-surface area of TE increased

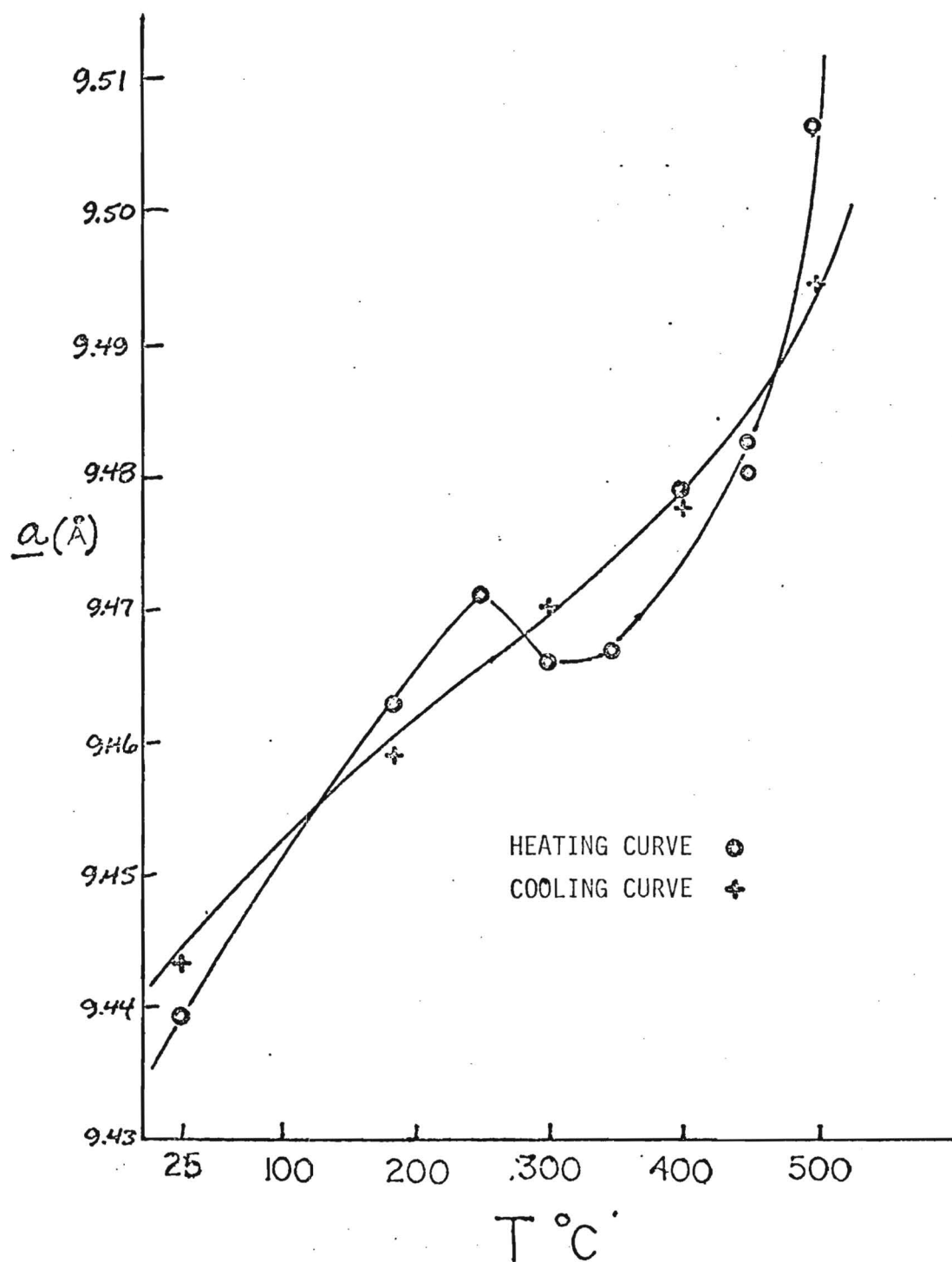


Figure 2

fourfold at 360°C presumably because of pyrolysis of the organic content, and to Zahradnik and Moreno's (1975) observation with isothermal water vapour sorption measurements that the "pore constrictions" are associated with the presence of organic-matter "plugs". Modification of the sample holder (e.g., higher sides and a small mesh screen covering the top) resulted in a much smaller weight loss at 410°C. The fact that the "spalling" of TE material occurs at such a well defined temperature and also the fact that with sufficient reduction of particle size a sharp weight loss is no longer seen suggest the existence of characteristic cavities within TE macro-structure similar to the cavities of Dibdin or pores of Moreno and Zahradnik. Furthermore, these observations suggest that the water vapor pressure at 410°C (~ 3380 p.s.i.) is a measure of the mechanical strength either of the TE macro-structure or of the "organic plugs" in the pores suggested by Zahradnik and Moreno.

The first slope of the TGA is the steepest and occurs in the temperature range 25 to 200°C. Maximum slope and gas emissions occur at 115°C. This first rapid loss (up to 0.8wt%) is generally accepted to be H_2O and assumed to be that adsorbed on the organic and/or inorganic component. We have found:

- 1) for human TE samples heated to less than 150°C the weight loss can be regained by exposure to atmosphere.
- 2) for TE heated to less than 500°C (but more than 150°C) the weight lost in the 25°C to 200°C range can only be partially regained by exposure to atmosphere.
- 3) if TE is heated to 1000°C the 25°C to 185°C weight loss can not be regained even after prolonged (4 months) exposure to atmosphere, or even 1 week in H_2O .
- 4) even hydrothermal treatment (200°C @ 350psi for 225 hours in H_2O) will not totally restore the weight loss in the 25-200°C range for TE which has been heated to 500°C.
- 5) storage of TE for 4 months over P_2O_5 removes 65% of material normally lost by 200°C.
- 6) storage of TE for 14 days at 110°C in vacuum removes 80% of the material normally lost by 200°C.
- 7) a reflux preparation of hydroxyapatite shows a TGA weight loss (0-200°C) of 0.4wt%.
- 8) a hydrothermal preparation of hydroxyapatite (500°C @ 17000psi in H_2O) shows no TGA weight loss in the range 0°C to 200°C.
- 9) deproteination of TE with hydrazine eliminates 40% of the weight loss seen in the TGA curve of untreated TE by 200°C.
- 10) light fraction TE. (i.e., specific gravity <2.8) has a larger TGA weight loss than the heavy fraction up to 200°C (~ 1 wt%) but deproteination eliminates 60% of this weight loss from the TGA curve.

Eighty per cent of the weight loss below 200°C is probably due to adsorbed water; half of which is associated with the organic, the other half with the inorganic. By 200°C the organic material is starting to denature which inhibits its ability

to readsorb water. Heating TE to 400°C has a considerable charring effect (sample turns grey and organic gases are evolved) and eliminates the ability of the organic material to adsorb water. The water adsorbed on the inorganic material is similar to that adsorbed on the reflux prepared hydroxyapatite (prepared at 100°C).

The second slope in the TGA curves of TE starts around 300°C and extends to 1000°C with a small inflection noted at 780°C. This weight loss is associated with:

- i) water (from inorganic and organic components)
- ii) CO₂ (from both inorganic and organic components)
- and iii) several unidentified organic species.

This weight loss (i.e., from 300°C to 1000°C) has a maximum weight loss rate and maximum gas emissions (as determined from dynamic evolved gas IR experiments) at 390°C. By 390°C some 2.5wt% has been lost as seen by TGA measurements. This maximum emissions at 390°C correlates well with the explosive scattering of enamel chips (~400μ) observed at 410°C. Part of this 2% weight loss between 300°C and 1000°C is associated with the organic component as can be seen by:

- i) the sample slowly gets darker as the temperature goes from 300°C to 800°C; but then turns white again by 1000°C.
- ii) deproteinization decreases the weight loss in the range up to 900°C by ~1wt%.
- iii) organic gases (as seen by dynamic evolved gas IR) are evolved over the entire temperature range of 300°C to 1000°C.

This weight loss due to the organic components above 300°C is fairly continuous and hence has a smoothing effect on the TGA curve. CO₂ gas (2320cm⁻¹) is evolved starting at 200°C and is also fairly continuous. Changes in the IR spectra of the carbonate region point to the initially incorporated carbonate as the source of the evolved CO₂. The remainder of the 2wt% loss between 300°C and 1000°C is primarily water.

With the complementary use of evolved gas-IR we have established that assay for water in TE by TGA alone will be in serious error for at least two reasons:

1) Water is lost continuously and in combination with other entities as the temperature is raised, and

2) As much as 20% of the water in TE may not leave the enamel but becomes incorporated as structural OH in the apatite portion (e.g., see LeGeros, 1973, who showed structural OH increased with heating).

From this point of view, TGA although useful, is not our most valuable tool because of the complex nature of the weight loss. We have thus started using the dynamic evolved gas IR analysis technique to study the evolved gases of TE as they are given off. This should give us more accurate numbers for the H₂O lost (or other species!).

Mass Spectrometry (MS) of Human TE

Mass spectrometry of TE samples for H₂O and CO₂ is confounded by these same two entities which occur as background. Secondly, although the organic components are a small weight per cent of our prepared TE, organic vapors with complex fragmenting patterns are a high percentage of the total weight lost in a MS run and constitute a confusing background which needs to be removed in order to study the potentially small amounts of the entities of interest.

PHOTOGRAPH LEGEND

Photo #1 Powder X-Ray Diffractometer and Environmental Chamber

1. Powder X-Ray Diffractometer
2. Environmental Chamber
3. X-ray Detector
4. X-ray Source

Photo #2 Close-up View of Sample Holder and Environmental Chamber Base-Plate

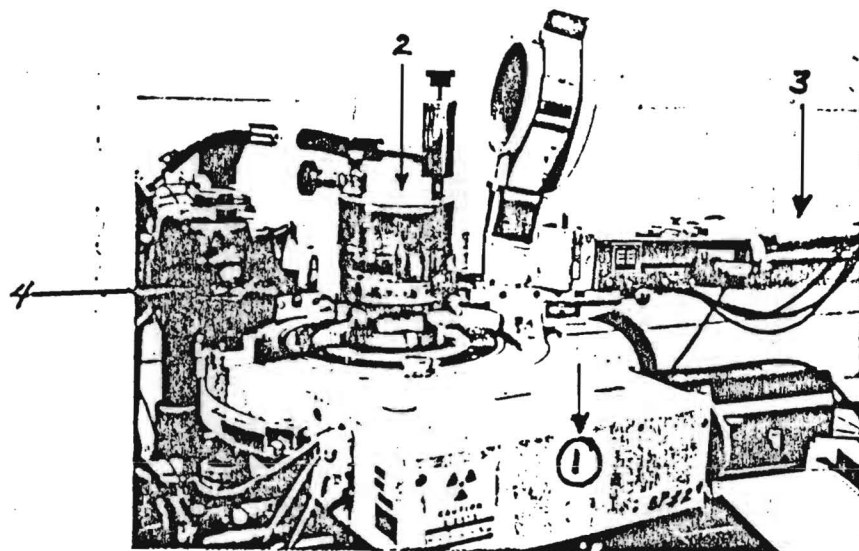
1. Powder Sample Holder with Heater Coils Imbedded
2. Water-cooled Base Plate
3. Adjusting Knob - to adjust position of sample in the x-ray beam
4. Wires for Heater Power and Thermocouple Readout

Photo #3 Environmental Chamber Base-Plate

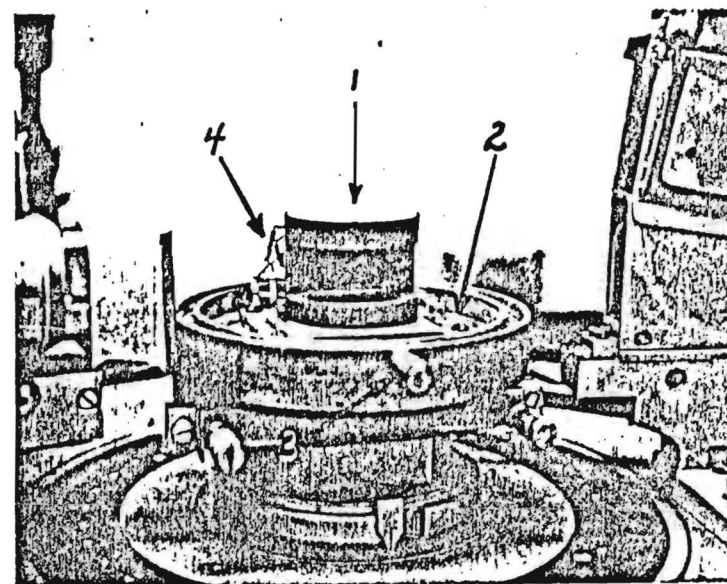
1. X-ray Source
2. Adjustable Platform on which Sample Holder is Positioned (see Photograph #2)
3. Connector Block for Heater-Power and Thermocouple Connections

Photo #4 Evolved Gas-IR Sample Holder

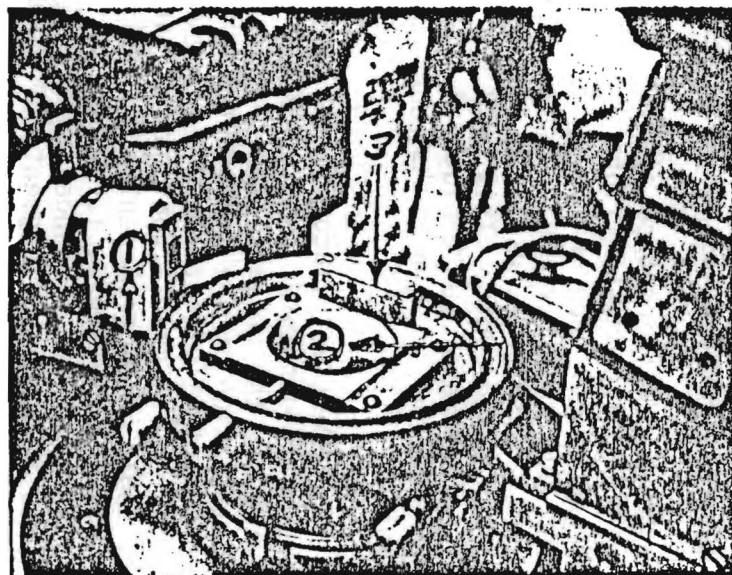
- 1 & 2. NaCl Windows - IR path is from 1 to 2
3. Heater Coil



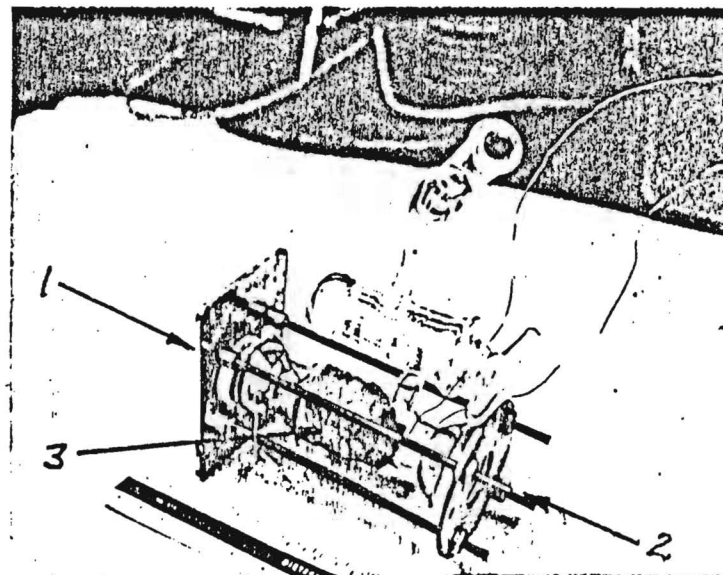
1
Powder X-Ray Diffractometer
and Environmental Chamber



2
Close-up View of Sample Holder and
Environmental Chamber Base-Plate



3
Environmental Chamber



4
Evolved Gas-IR Sample Holder

We are presently performing step-wise heating regimens of TE for MS and DGIR analyses. MS analysis is also being performed on evolved gases collected from the environmental chamber during x-ray powder diffraction runs.

The present technique of step-wise heating and then the static analysis by the sector type mass spectrometer available to us does not fully meet the needs of this project. The gases are not analyzed as they are emitted (i.e., dynamically as the temperature is changed) but are collected in a glass vessel, while the sample is held at a constant temperature, to be analyzed at a latter time. This procedure suffers from a number of problems. First, the quantitative information is compromised because some of the gases tend to condense out on the cool walls of the collection vessel. This changes the ratios of the various gaseous species present in the gas to be eventually injected into the mass spectrometer. Secondly, with the mass spectrometer available to us, the injected gas must follow a path with some bends in it before it arrives at the analyzing magnet. At each bend, the various gaseous species will be removed from the gas stream (e.g., by condensation or scattering) to varying degree for each specie, further compromising the quantitative aspects of the data collected. A third problem is that those in charge of this instrument do not want us to inject gases at temperatures higher than about 300°C at the inlet. This is to reduce the possibility of contaminating the system with heavy organic mass fragments with a resulting costly down time to break open the vacuum system and thoroughly clean the system. A quadra-pole mass spectrometer, with its straight path through the system, reduces or eliminates the problems mentioned above. The gaseous effluents can be analyzed dynamically (i.e., on-line as the temperature is varied without the intermediate step of a collection vessel), the data collected would be more quantitative because of fewer opportunities for the gas stream to interact with various parts of the equipment along the path (it follows that the problem of contamination would also be reduced), and higher inlet temperatures for the injected gas would be feasible.

Several different possibilities for using quadra pole type MS's were checked out. A Bendix time-of-flight unit in Ceramic Engineering needed repairs which would cost more than acquiring a new unit (~\$10000). A residual gas analyzer in the Physics department was in dedicated use and unavailable for use by this project. Similarly, use of a quadra pole MS in the Areospace Engineering department was looked into. This unit was being used intensively and it was feared that injection of our biological samples at high temperatures would result in contamination and, hence, shut down the unit for extended lengths of time for cleaning.

To effectively, acquire the dynamic (and quantitative!) data of mass fragments vs temperature, a mass spectrometer, of the quadrapole type, needs to be acquired by the project (see the budget for the first year). Mass spectrometer identification of the various enamel effluents at each temperature has become more important with the result from dynamic evolved gas i.r. that the several evolved species are given off continuously and simultaneously. Good quantitative MS data would both complement and provide a check on the dynamic evolved gas i.r. results. For example, i.r. band assignments could be made by correlating changes in i.r. bands (e.g. changes in areas and shifts in position) with quantitative changes in the mass fragments of the MS output.

Infra-Red(IR) and Dynamic Evolved Gas IR (DGIR) of Human TE

With the realization that the TGA curves of TE were a composite of simultaneous continuous emissions of several species, the sample chamber (or cell) for continuous monitoring of the IR absorption bands of evolved gases was designed and built (see the next section: "Equipment Design, Fabrication and Modification"). Thus far, nine major absorption bands have been noted, as well as, many small peaks in the organic "Fingerprint" region ($600-1500\text{cm}^{-1}$). Present efforts are directed toward calibrating the cell with pure oxalates in an effort to obtain weight loss vs temperature curves for each major specie evolved. This technique, DGIR, is presently being investigated as a potential analytic assay for water. The only bands of the 9 assigned with certainty are H_2O and CO_2 which are the largest. Several other bands are assigned to at least two different organic species (one a gas and the other a condensed vapor).

Equipment Design, Fabrication and Modification

Several pieces of equipments were designed and built for DE04151. As mentioned in the section on x-ray diffraction, a sample environmental chamber (see Photos 1 through 3) was built to enable the sample to be heated up to 500°C while maintaining the sample in a vacuum or some control atmosphere. This chamber was used to obtain the TE (under vacuum) data vs temperature used in the PFSR studies. It will be further used in DE04151-03 to maintain the sample at humidities other than ambient.

A special sample chamber (see photo #4) was constructed such that various species of the evolved gases could be monitored by IR continuously as the temperature of the sample was increased. This chamber has been used extensively in the dynamic pyrolysis studies of human TE (see R.A. Young et al. "Dynamic Pyrolysis Studies of Human Tooth Enamel", AADR, Las Vegas, June 1977).

A4d) Published Abstracts of Oral Presentations at Scientific Meetings

- i) "Experience with x-Ray PFSR: Profiles, LaPO_4 , and Tooth Enamel", P.E. Mackie, Dennis B. Wiles and R.A. Young, Program and Abstracts, American Crystallographic Association, Series II, 5 42, (1977).
- ii) "Preliminary Crystal Structure Analysis of Powdered Human Tooth Enamel", P.E. Mackie and R.A. Young, J. Dent. Res., 56, (Special Issue B), B 232 (1977).
- iii) "Dynamic Pyrolysis Studies of Human Tooth Enamel", R.A. Young, Derrold W. Holcomb and P.E. Mackie, J. Dent. Res., 56 (Special Issue B), B 233 (1977).

Mackie, Paul E.
209-32-0029

A4e) Staffing

Paul E. Mackie, Senior Research Scientist Engineering Experiment Station	1 June 1975 - 31 May 1977
R.A. Young, Principal Research Scientist Engineering Experiment Station	1 June 1975 - 31 May 1977
D.W. Holcomb, Assistant Research Scientist Engineering Experiment Station	1 July 1976 - 31 May 1977
Graduate Research Assistant Engineering Experiment Station	1 Jan 1976 - 1 June 1975
J.R. Cagle, Assistant Research Scientist Engineering Experiment Station	1 June 1975 - 31 May 1977

B. Specific Aims*

To further improve our knowledge of the role of water in human tooth enamel by :

- 1) refining the assay techniques for water by TGA, IR, PFSR and dynamic evolved gas IR analyses developed in DE04151 years 1 through 3.
- 2) developing atomic-scale detailed models for the incorporation, mobility and changeability of various water species in tooth enamel.
- 3) determining how atomic-scale detail of TE (with particular emphasis on 'water') varies or correlates with various selected parameters (e.g., age, density, carious character, color, white spots, etc.).

C. Methods of Procedure

C1. Sample Collection

Teeth will be collected from local dental clinics. Both pooled and classified teeth will be collected. Initial classification of the teeth into three ages groups (15 years and under, over 50 years old, and 16-49 year) will be made at the collection point by the oral surgeons. Further classification

*N.B. These aims are necessarily similar to those of the original project period, because of both 1) the comprehensive nature of the aims in this project area and 2) the reduction of effort noted at the beginning of the Comprehensive Progress Report (section A4).

of the teeth into subgroups (e.g., type of teeth, carious or noncarious, etc.) will be made by dental personnel working on the project and working as consultants.

C2. Tooth Handling and Powder Preparation

A few sound teeth will be set aside for sectioning for SEM work. The remainder will be used to form the "pooled" enamel powder. (Pooling is necessary in view of the quantities needed, especially for x-ray (up to 1 gm) and neutron (up to 15 gm) diffraction.) The word "pooled" is used here in the sense that some variables (e.g., sex, age within the age bracket, tooth type, fluoride environment, CO₂ content, etc.) will be averaged in the process of generating the enamel powder from the supply of teeth. The teeth will be cleansed by rinsing in distilled water and the pellicule removed by a light burnishing of the surface. The crowns will then be separated from the roots and the dentine ground away from the crowns. The crowns will then be crushed and the powder examined under a low power microscope and ultraviolet illumination for fluorescence indicative of remaining dentine. Particles fluorescing will be removed. Fractions of the enamel with various densities will be obtained with the technique of flotation in liquids of different densities (e.g., in tetrabromoethane to obtain enamel with a specific gravity 2.95).

C3. Pretreatments

Before the main parts of the experimental procedures are carried out, some enamel samples will be subjected to various pre-treatments (e.g., heating, relative humidity adjustment, chemical treatment, deuteration, etc.). These pre-treatment (or pre-conditioning) will be used to obtain various standard conditions prior to the actual experimental procedures.

C4. Analytical Techniques

The main techniques to be employed are x-ray diffraction, infra-red spectroscopy, dynamic evolved gas infra-red spectroscopy and thermogravimetric analysis. Additional techniques to be used as time and money permit are neutron diffraction, mass spectrometry and nuclear magnetic resonance.

C4a. X-ray and Neutron Powder Diffraction Studies (XRD, ND)

In these experiments (performed on human TE) we will (1) make precision measurements of the lattice parameters as a function of temperature and as a function of humidity at room temperature, (2) detect and identify any other crystalline phases which may occur during these temperature and humidity treatments, and (3) perform pattern-fitting-structure-refinements with the powder diffraction data. The samples to be examined will be those which have had the same pre-treatments as those used in the IR and dynamic evolved gas IR (DGIR) experiment. There are several goals we can expect to attain from these diffraction experiments:

(1) From the DGIR experiments we will know at what stages in the heating programs the various effluents appear. Lattice parameter measurements (especially a) will tend to indicate whether or not that effluent is part of the crystal structure rather than a part of the enamel incorporated at a higher level of structure organization.

(2) The analyses of the powder diffraction patterns (collected at approximately 50°C increments from room temperature to 500°C and at several different relative humidities at room temperature) will permit identification of other crystalline phases and, with use of an internal standard, indicate the amount of any amorphous content. The primary interest in these various components of enamel, crystalline or amorphous, being their water content and how they may effect the various assay techniques for water.

(3) The pattern-fitting-structure-refinement (PFSR) method (a new and very promising analytical technique for analyses of powder diffraction data) will permit the refinement of various atomic-scale structural models to the purpose of determination of how water is incorporated in the crystal (if indeed we find from concomitant lattice parameter changes that it is in the crystal). In as much as the other effluents of TE may affect our determination of how water is incorporated in the inorganic phase of enamel, this project will depend heavily on the results of NIDR project DE 01912 (DE 04151 and DE 01912 share laboratory and office space and in several instances personnel.) This technique applied to x-ray data is more effective for the heavier effluents (the "tracks" of those lighter effluents can be followed to some degree by observing their effect with PFSR on the remainder of the structure). However, for the lighter effluents (such as H,OH,H₂O and H₃O) the same technique will be more effectively applied with neutron powder diffraction data. Neutron diffraction will be used sparingly since the sample requirements are very high (15 grams, or the dense-fraction enamel harvest of about 150 teeth) and neutron beam charges are expensive.

C4b. Infra-Red Spectroscopy (IR) and Dynamic Evolved Gas IR (DGIR)

Infra-red spectra will be collected from samples having had the same pre-treatment as those samples used in the TGA and x-ray diffraction experiments. Bartlett and Young (1972), among many others, have shown that with the proper precautions during the preparation of the sample in a KBr pellet, atmospheric moisture can be effectively excluded from apatite specimens prepared for IR studies. Using the techniques they (Bartlett and Young, 1972) used, one can do quantitative IR analysis for OH in its structural location in hydroxyapatite and, to some extent, for H₂O. In the DGIR experiments, several different IR bands will be followed as the sample is treated and in this manner the weight change observed with the TGA experiments will be apportioned to the various effluents identified so that an accurate assay for water will be obtained.

C4c. Weight Change vs Heating

The various samples will be heated at several different temperatures (~50°C intervals up to 1000°C and held at one temperature until constant weight is achieved) and the weight changes recorded. In conjunction with DGIR, XRD, ND and IR data, these data will be used to quantify (weight %) the contributions to the weight loss of the various volatile constituents at each stage in the heating program.

D. Significance

To have a chemical understanding of the mechanisms of tooth properties in health and in disease, one must have (as a minimum) a knowledge of the structural relationships and roles of the major constituents in tooth enamel. Water, present at 2 to 7 wt%, is a significant constituent about which not much is known (cf. the knowledge of the crystalline component, apatite). In this work, we propose to study those aspects of water in enamel which will provide a foundation for the understanding of the role(s) of water in human tooth enamel. The study will involve a coordinated approach in which use will be made of several complementary techniques, both established (e.g., x-ray and neutron diffraction, IR, etc.) and new (e.g., the powerful new technique of pattern-fitting-structure-refinements of powder diffraction data), to explore the applicability of various models for the inclusion of water in enamel.

E. Facilities Available

All required facilities, including major equipment (with the exception of the quadrupole mass spectrometer requested in the first year's budget), laboratory space and office space, are available. The major equipment items include those for computer-controlled or assisted powder x-ray diffractometry, a versatile computer-controlled single-crystal and powder neutron diffraction unit operating at a major research reactor (5 megawatt heavy-water moderated), large and small computer facilities, access to infrared and laser-Raman spectroscopy facilities on campus, small chemistry laboratory especially equipped for work on apatites and tooth enamel and a major library.

F. Collaborative Arrangements

The proposed project is not critically dependent on any formal collaborative arrangements. Dr. Howard Myers, who did some of the stimulating early studies of water in tooth enamel and is very well known in dental-research circles, is presently serving as a consultant to DE04151 and has agreed to continue on with the renewal project. Dr. Myers is headquartered in Philadelphia.

G. Principal Investigator Assurance

The undersigned agrees to accept responsibility for the scientific and technical conduct of the research project and for provision of required progress reports if a grant is awarded as the result of this application.

Date

Principal Investigator